N 62 65877

MR February 1944

NATIONAL ADVISORY COMMITTEE FOR AERONAUTICS

WARTIME REPORT

ORIGINALLY ISSUED
February 1944 as
Memorandum Report

THE EFFECTS OF A HIGHLY CAMBERED LOW-DRAG WING AND OF AUXILIARY FLAPS ON THE HIGH-SPEED AERODYNAMIC CHARACTERISTICS OF A TWIN-ENGINE PURSUIT AIRPLANE MODEL

By Victor M. Ganzer

Ames Aeronautical Laboratory
Moffett Field, California

NACA

WASHINGTON

NATIONAL ADVISORY COMMITTEE FOR AERONAUTICS

MEMORANDUM REPORT

for the

Air Material Command, U. S. Army Air Forces

THE EFFECTS OF A HIGHLY CAMBERED LOW-DRAG WING AND OF AUXILIARY FLAPS ON THE HIGH-SPEED AERODYNAMIC CHARACTERISTICS OF A TWIN-ENGINE PURSUIT AIRPLANE MODEL

By Victor M. Ganzer

SUMMARY

This report presents the results of tests of a model of a twin-engine pursuit airplane. Two wings were investigated, an NACA 230-series wing and a highly cambered NACA 66-series wing. Auxiliary control flaps were tested in combination with each of the wings.

Data showing the comparison of the high-speed aerodynamic characteristics of the model when equipped with each of the wings, the effect of the auxiliary control flaps on the aerodynamic characteristics, and the elevator effectiveness for the model with the 66-series wing are presented.

INTRODUCTION

A model of a twin-engine pursuit airplane was tested previously in the high-speed wind tunnel at the Ames Aeronautical Laboratory to determine, among other things, the relative merits of an NACA 230-series wing and an NACA 66-series wing cambered for an optimum lift coefficient of 0.1 at the root (reference 1). Results of that investigation led to the belief that a more highly cambered 66-series wing might extend the usable Mach number range for the airplane even more than did the low-cambered wing.

Tests of a similar airplane model at high speed indicated that auxiliary control flaps were effective in producing forces and moments tending to pull the airplane out of high-speed dives (reference 2). It was desired to determine if such auxiliary control flaps would be effective on the model reported on herein and, if so, the optimum location of the flaps.

The specific purposes of the present investigation were as follows:

1. To compare the high-speed aerodynamic characteristics of the model having an NACA 230-series wing with those of a model having a highly cambered NACA 66-series wing

2. To determine the effectiveness, in producing pull-out forces and moments, of auxiliary control flaps in combination with the 230-series wing

3. To determine the effectiveness, in producing pull-out forces and moments, of auxiliary control flaps in combination with the highly cambered 66-series wing

4. To determine the variation of elevator effectiveness with Mach number for the model equipped with the highly cambered 66-series wing

The investigation was conducted in the Ames 16-foot high-speed wind tunnel at the request of the Air Material Command, U. S. Army Air Forces.

APPARATUS

A description of the model with the NACA 230-series wing and the large booms may be found in reference 1. The large booms were used in all of the present tests. A three-view drawing of the model is shown in figure 1 and a photograph of the wind-tunnel setup in figure 2. Some of the pertinent dimensions are given in the following table:

	230-series wing	Highly cambered 66-series wing
Wing area, sq ft	16.67	16.67
Mean aerodynamic chord, ft	1.525	1.525
Horizontal tail area, sq ft	3.623	3.623
Elevator area, sq ft	0.903	0.903
Tail length, 25 percent M.A.C. to elevator hinge line, ft	4.979	4.979
Wing section (constant chord part of wing)	NACA 23016	NACA 66,2-416 (a = 0.5)
Wing section, tip (2.17 in. inboard from wing tip)	NACA 4412	NACA 66,2-616 (a = 0.5)
Incidence, constant chord part of wing, degrees	2°	0°
Incidence, tip section	0°	0°
Stabilizer incidence	2°	0° and 2° (noted in figures)

Each of the auxiliary control flaps had a span of 12 inches and a constant chord of 1.82 inches (10 percent of the M.A.C.). The outboard flaps were mounted just outboard of the booms, as shown in figure 3; the inboard flaps between the booms and the fuselage. The hinge line was located at the various chordwise positions noted in the figures. The flap angle indicated was the angle between the flap and the lower surface of the wing.

SYMBOLS

Symbols used in this report are defined as follows:

V free-stream velocity, feet per second

q	free-stream dynamic pressure $\left(\frac{1}{2}\rho V^2\right)$, pounds per square foot
M	Mach number $\left(\frac{V}{\text{velocity of sound}}\right)$
S	wing area, square feet
M.A.C.	mean aerodynamic chord, feet
C_L	lift coefficient $\left(\frac{\text{lift}}{qS}\right)$
C_D	drag coefficient $\left(\frac{\text{drag}}{qS}\right)$
$C_{m_{c.g.}}$	pitching-moment coefficient $\left(\frac{\text{pitching moment about the center of gravity}}{qS \text{ M.A.C.}}\right)$
c_n	section normal-force coefficient $\left(\frac{\text{section normal force}}{qSc}\right)$ (Positive when acting upward.)
c	section chord, feet
α	angle of attack measured from the fuselage reference line, degrees
ΔC_L	increment of lift coefficient due to the extension of the auxiliary flaps
ΔC_D	increment of drag coefficient due to the extension of the auxiliary flaps
ΔC_m	increment of pitching-moment coefficient due to the extension of the auxiliary flaps or to the deflection of the elevator
P	pressure coefficient $\left(\frac{\text{local static pressure - free-stream static pressure}}{q}\right)$
P_{cr}	value of P at which the local velocity reaches the local velocity of sound

M_{cr} value of M at which the local velocity reaches the local velocity of sound

δ_e elevator deflection, degrees (Positive when the trailing edge moves down.)

i_t stabilizer angle of incidence, degrees (Measured from the fuselage reference line.)

g acceleration of gravity, feet per second per second

Subscripts

U upper surface

L lower surface

RESULTS

Correction of Data

The same tare forces and moments and tunnel-wall corrections were applied to the data as were used in the previous report on the model (reference 1). The tunnel-wall corrections were as follows:

Angle-of-attack correction (deg) = 0.629 C_L

Drag-coefficient correction = 0.01097 C_L^2

Pitching-moment-coefficient correction = 0.0155 C_L

No corrections for flow inclination or constriction were applied.

Presentation of Results

The results of the force and pressure measurements on the complete model with the 230-series wing and with the highly cambered 66-series wing are found in figures 4 to 10.

Data obtained from tests of auxiliary flaps on the 230-series wing are found in figures 11 to 19 and from tests of flaps on the 66-series wing in figures 20 to 27.

Data obtained from tests with the elevator deflected and from tests with the two stabilizer angles are shown in figures 28 and 29.

DISCUSSION

Comparative Characteristics of Model with NACA 230-Series Wing and of Model with Highly Cambered NACA 66-Series Wing

As shown in reference 1, the increase of static longitudinal stability, the shift of the lift coefficient for balance at constant elevator angle, and the reduction of the maximum lift coefficient at speeds above the critical seriously limit the speeds to which the airplane with the 230-series wing could be dived safely. The substitution of a 66-series wing, cambered for a lift coefficient of 0.1 at the root, extended by approximately 50 miles per hour the speed at which pull-outs from dives could be made without these changes of stability and lift coefficient for balance; but the maximum lift coefficient was considerably reduced at the test Reynolds numbers. It was suggested in reference 1 that a more highly cambered 66-series wing should make a greater maximum lift coefficient available than did the low-cambered 66-series wing, and might further increase the speed from which normal pull-outs from dives could be made.

The lift, drag, and pitching-moment characteristics of the model with the 230-series wing and with the highly cambered 66-series wing are shown in figures 4 to 6. As indicated in reference 1, high-speed longitudinal-control difficulties arise mainly from the increase of static longitudinal stability and the decrease of the lift coefficient for balance as the critical Mach number is exceeded. Figure 4(a) shows that the static longitudinal stability, $-\partial C_m/\partial C_L$ of the model with the 230-series wing, increased from 0.085 at a Mach number of 0.491 to approximately 0.47 at a Mach number of 0.747, an increase of 450 percent. Through the same Mach number range the lift coefficient for balance with the elevator neutral decreased from 0.7 to 0.17.

The model equipped with the highly cambered 66-series wing experienced an increase of static longitudinal stability of only about 60 percent when the Mach number increased from 0.491 to 0.747 (fig. 5). This lesser change of stability should make the airplane with the highly cambered wing more controllable at high Mach numbers than it would be with the 230-series wing. The substitution of the 66-series wing also reduced the change of balance with Mach number. With this wing the lift coefficient for balance decreased from 0.65 at a Mach number of 0.491 to 0.3 at a Mach number of 0.747.

Figures 7(a) to 7(d) compare, directly, the aerodynamic characteristics of the models equipped with the two wings. It is evident from figure 7(c) that at lift coefficients of 0.5 and 0.7 the highly cambered 66-series wing resulted in less drag at high Mach numbers, while at a lift coefficient of 0.1 (fig. 7(b)) the model equipped with the 230-series wing showed less drag. Figure 7(d) shows that the model equipped with the 66-series wing attained higher Mach numbers before marked changes in the lift coefficient for balance or the static longitudinal stability occurred, especially at lift coefficients of 0.3, 0.5, and 0.7; these changes in lift coefficient and stability are indicated when the pitching-moment coefficient for a constant lift coefficient diverges sharply.

Pressure distributions over the 66-series wing are shown in figure 8; pressure distributions for the 230-series wing may be found in reference 1. Figure 9, which shows the critical Mach numbers of the wings as determined from the pressure distributions, illustrates the fact that the critical speed of the highly cambered 66-series wing was greater than that of the 230-series wing at positive angles of attack. The difference amounted to an increase of critical Mach number of about 0.125 at an angle of attack of 4° or to about 90 miles per hour at 20,000 feet altitude.

Figure 10 shows a comparison of selected characteristics for the 230-series wing, the low-cambered 66-series wing (reference 1), and the highly cambered 66-series wing. The Mach number at which the pitching-moment coefficient begins to decrease, when plotted as in figure 7(d), is considered the limiting usable Mach number; because if this Mach number were exceeded the decrement of the pitching-moment coefficient (coupled with the increase of static longitudinal stability) would make pull-outs from dives difficult. The model, when equipped with the highly cambered 66-series wing, had a higher limit of usable Mach numbers at lift coefficients above 0.1 than it did when equipped with the 230-series wing, and a higher limit for lift coefficients above 0.6 than did the model when equipped with the low-cambered 66-series wing. The maximum lift coefficient at a Mach number of 0.6 with the highly cambered 66-series wing was especially noteworthy, being about 1.34 as compared to 1.1 for the 230-series wing and 0.89 for the low-cambered 66-series wing (fig. 10). These maximum lift coefficients correspond to the following normal accelerations at various altitudes:

Altitude (ft)	Maximum acceleration, g, M = 0.6.		
	Highly cambered 66-series wing	230-series wing	Low-cambered 66-series wing
40,000	2.24	1.83	1.48
30,000	3.57	2.93	2.37
20,000	5.54	4.55	3.68
10,000	8.27	6.79	5.50

This additional maximum lift coefficient is especially valuable for a high-altitude fighting airplane which may be required to develop large accelerations at high speed.

Auxiliary Control Flaps in Combination With the 230-Series Wing

Wind-tunnel tests of other models (reference 2) indicate that auxiliary control flaps of the type used in this test usually cause forces and moments to be developed which produce positive normal accelerations. The results of reference 1 and of the present tests indicate that the airplane will develop moment and stability changes at high Mach numbers which will oppose recovery from high-speed dives. The use of auxiliary control flaps should provide additional control for recovery from such dives.

Experience indicates that the use of flaps on the wing near the center of the span may result in tail buffeting and shaking. Because of this consideration, most of the flaps tested in this investigation were installed outboard of the booms where the wing wake would have less effect on the tail.

Figures 11 to 16 show the additional pitching-moment coefficient and drag coefficient which resulted from the flaps at various locations. Using the criteria that the requirement for auxiliary control flaps is the development of positive (climbing) moments when the flaps are deflected, an analysis of the figures indicates that the 20-percent-chord location is the best location for the outboard flaps, and that a 45° flap opening gave almost as much additional pitching moment as did the 60° opening. Lift, drag, and pitching-moment characteristics of the model with the outboard 45° auxiliary flaps at 20 percent of the wing chord are presented in figure 17, and wing and flap pressure distributions are presented in figure 18. The figures show that at low lift coefficients positive pitching-moment-coefficient increments of as much as 0.1 may be expected from the use of these flaps. Assuming that the deflection of the flaps would have no effect on the floating angle of the elevator and using the data presented in figures 4(a) and 17, if the airplane were trimmed in a steady glide at a Mach number of 0.747 at 20,000 feet altitude (C_L approximately 0.14), the extension of the flaps would produce a normal acceleration of about 1.9g with no force on the stick.

Section normal-force coefficients with the flaps retracted and with the flaps open are plotted in figure 19. These coefficients were obtained from the pressure distributions. The actual magnitude of the coefficients may be subject to some error, as the complete pressure distributions were faired from data obtained at only six points on each surface of the wing. However, the data show that the total section normal-force coefficients increased markedly when the flaps were deflected, especially at the higher Mach numbers and, as one would expect, the flaps affected the pressures on both the upper and lower surfaces of the wing. The data from force tests also show an increase of the effectiveness of the flaps at the high Mach numbers (fig. 11).

Auxiliary Control Flaps in Combination With the Highly Cambered 66-Series Wing

Tests of auxiliary control flaps outboard of the booms on the highly cambered 66-series wing showed that negative (diving) moments resulted from the flaps at high Mach numbers, rather than the desired climbing moments (fig. 20). Figures 19 and 22 to 24 show that the effect of the outboard flaps on the section normal-force coefficient, on the total lift coefficient, and on the moment of the wing was quite similar for the 230-series wing and for the highly cambered 66-series wing; hence it is surprising that the effectiveness of the flaps in producing positive pitching moments was not similar. It is possible that the difference in flap effectiveness was due to a difference in their effect on the downwash at the tail resulting from a difference in lift distribution.

The auxiliary control flaps mounted inboard of the booms on the 66-series wing gave the desired climbing moments. Data obtained from tests of inboard flaps at several flap angles are shown in figures 25 and 26, and the lift, drag, and pitching moment characteristics of the model with the inboard flaps at 30 percent chord at 30° are shown in figure 27. The climbing moment with the inboard flaps was undoubtedly due to the increased downwash at the tail caused by the increase of lift coefficient on that part of the wing just ahead of the tail.

Elevator Effectiveness

The effect of elevator deflection on the pitching-moment coefficient was determined for the model equipped with the highly cambered 66-series wing. The results of the tests with the elevator deflected are found in figure 28. The effectiveness of the elevator decreased as the Mach number increased above 0.7. The elevator effectiveness as determined with the 230-series wing on the model did not decrease appreciably as the Mach number exceeded 0.7, as is shown in reference 1. No reason for the loss of elevator effectiveness with the 66-series wing on the model is readily apparent, especially since the stabilizer effectiveness dC_m/di_t did not change appreciably as the Mach number increased (fig. 29).

CONCLUDING REMARKS

1. The high-speed aerodynamic characteristics of the model were improved by the substitution of a highly cambered NACA 66-series wing for an NACA 230-series wing, especially with regard to the maximum lift coefficient at Mach numbers of about 0.6 (1.34 for the 66-series wing as compared to 1.1 for the 230-series wing), and the lift coefficient available for pull-outs from high-speed dives (0.56 for the 66-series wing as compared to 0.18 for the 230-series wing at a Mach number of 0.7).

2. The use of auxiliary control flaps on the 230-series wing, either outboard or inboard and outboard of the booms, resulted in forces and pitching moments which would tend to pull the airplane out of high-speed dives. The test results indicated that the extension of the outboard flaps at 20 percent of the wing chord to an angle of 45° would produce a normal acceleration of about 1.9g from a steady glide at a Mach number of 0.75.

3. Auxiliary control flaps inboard of the booms on the highly cambered 66-series wing were effective in producing forces and moments tending to pull the airplane out of high-speed dives, but flaps mounted outboard of the booms were not effective.

4. The elevator effectiveness when the model was equipped with the highly cambered 66-series wing decreased as the Mach number increased above 0.7.

Ames Aeronautical Laboratory,
National Advisory Committee for Aeronautics,
Moffett Field, Calif.

REFERENCES

1. Ganzer, Victor M: High-Speed Wind-Tunnel Tests of a 1/6-Scale Model of a Twin-Engine Pursuit Airplane. NACA CMR, Dec. 1942.

2. Erickson, Albert L: Wind-Tunnel Investigation of Devices for Improving the Diving Characteristics of Airplanes. NACA CMR No. 3F12, 1943.

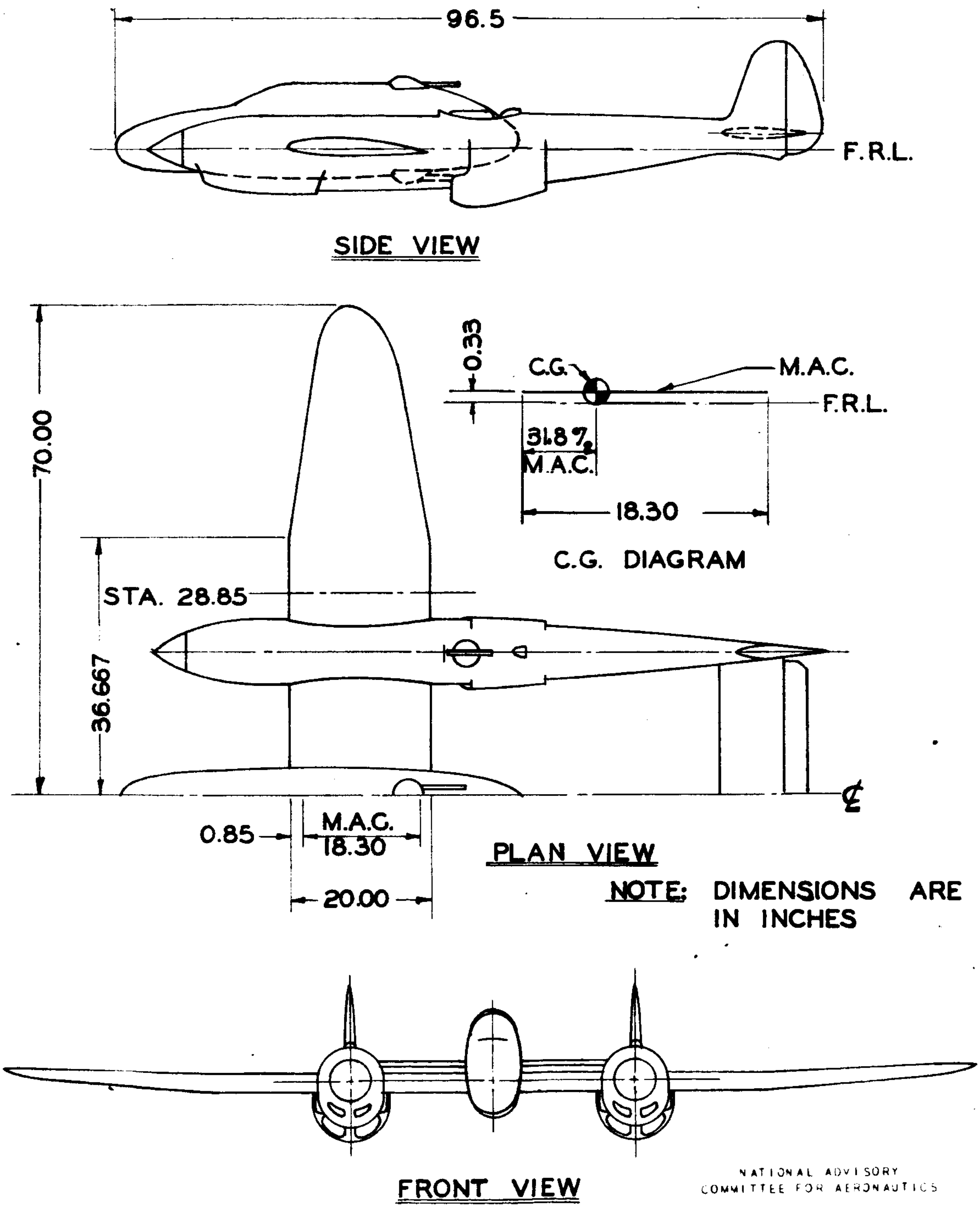

FIGURE 1.- THREE VIEW DRAWING OF THE $\frac{1}{6}$-SCALE MODEL OF A TWIN-ENGINE PURSUIT AIRPLANE.

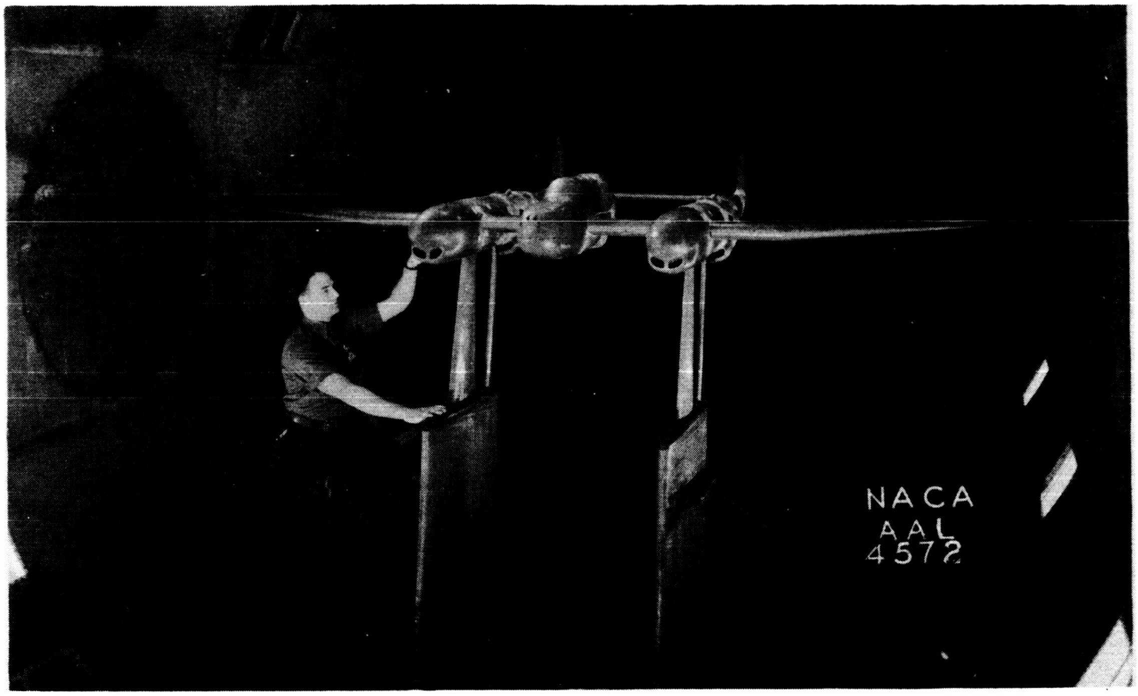

Figure 2.- The 1/6-scale model mounted in the 16-foot wind tunnel.

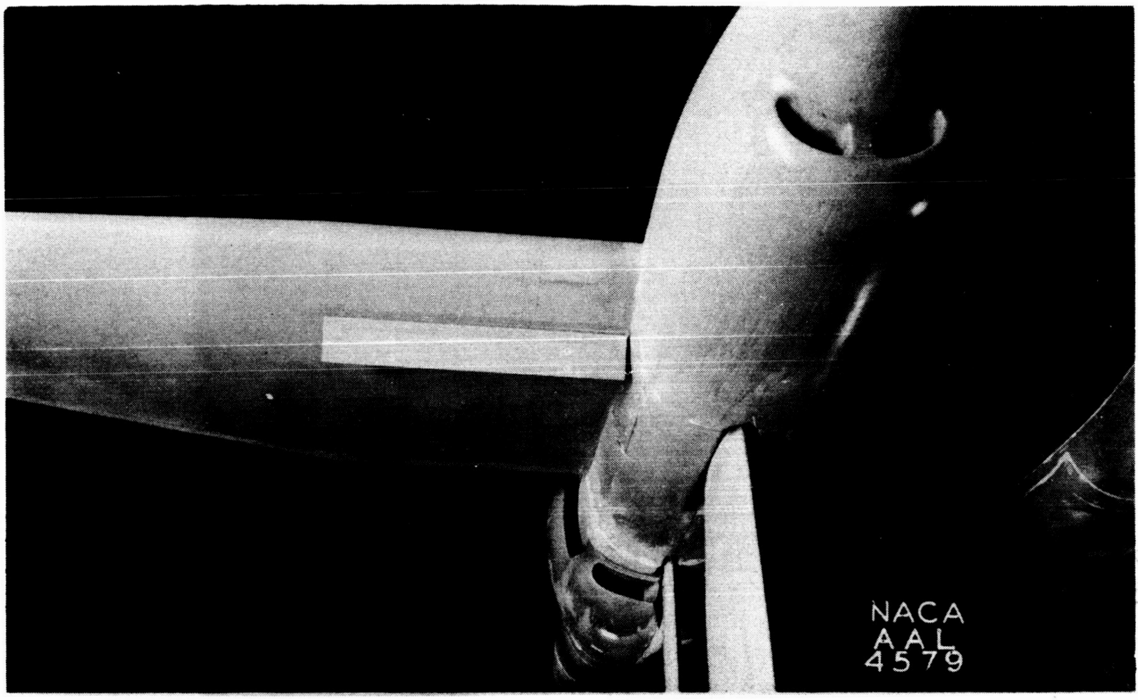

Figure 3.- View from below of the outboard 60° auxiliary control flap at 20-percent wing chord.

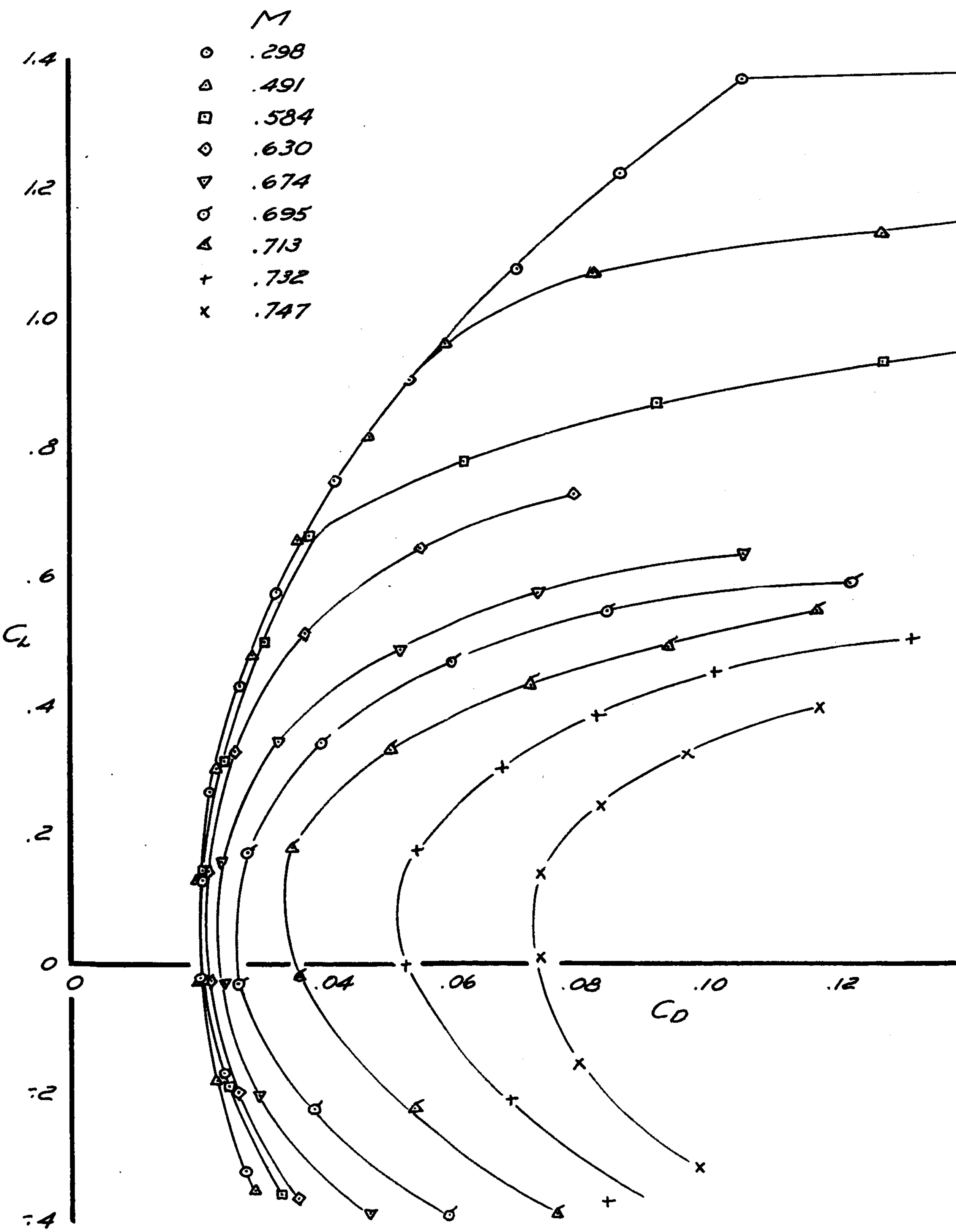
M
.298
.491
.584
.630
.674
.695
.713
.732
.747
1.4
1.2
1.0
.8
.6
.4
.2
0
-.2
-.4
C_L
0
.04
.06
.08
.10
.12
C_D

FIGURE 4A

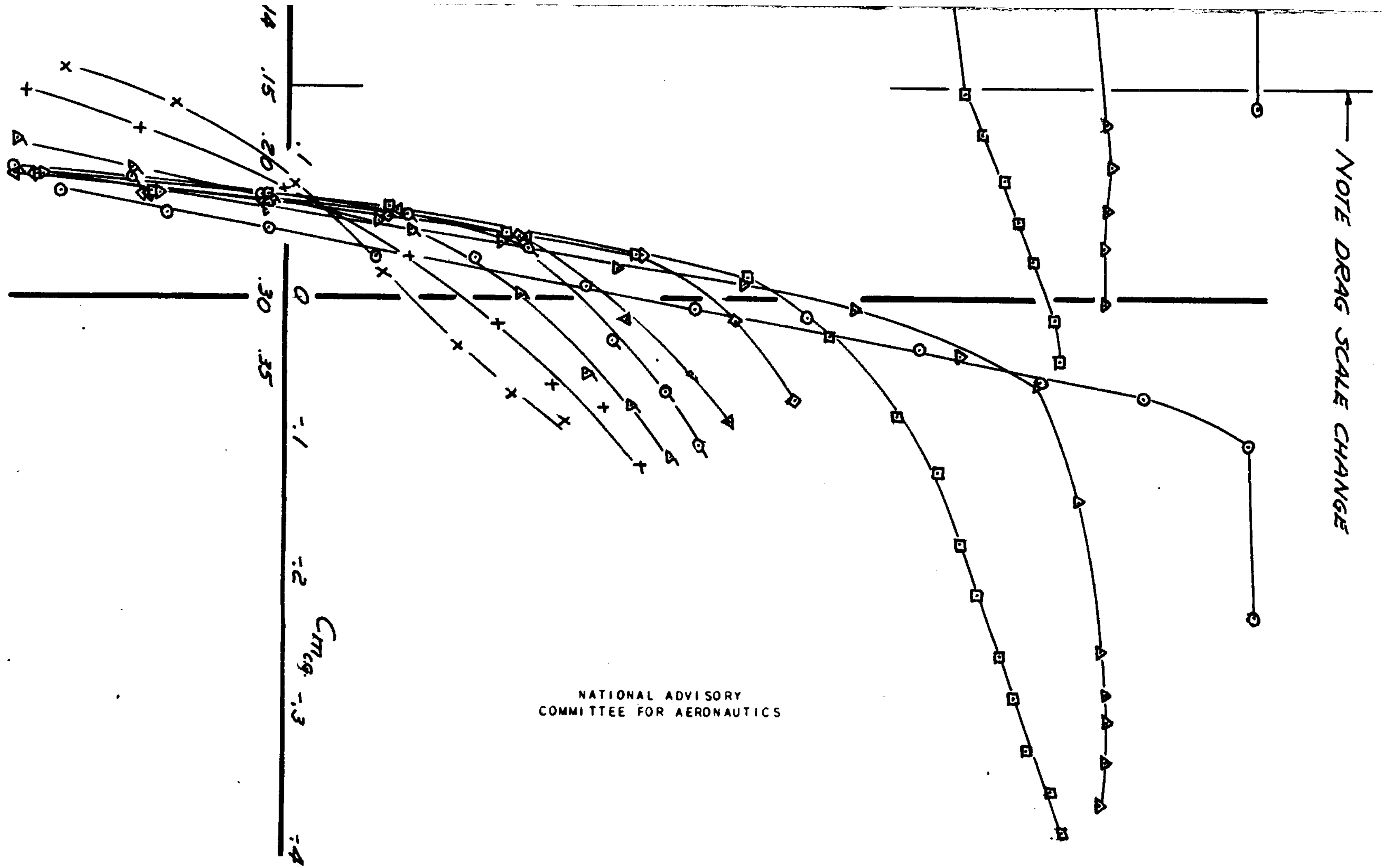

FIGURE 4B. - DRAG AND PITCHING-MOMENT CHARACTERISTICS OF THE MODEL WITH THE NACA 230-SERIES WING.

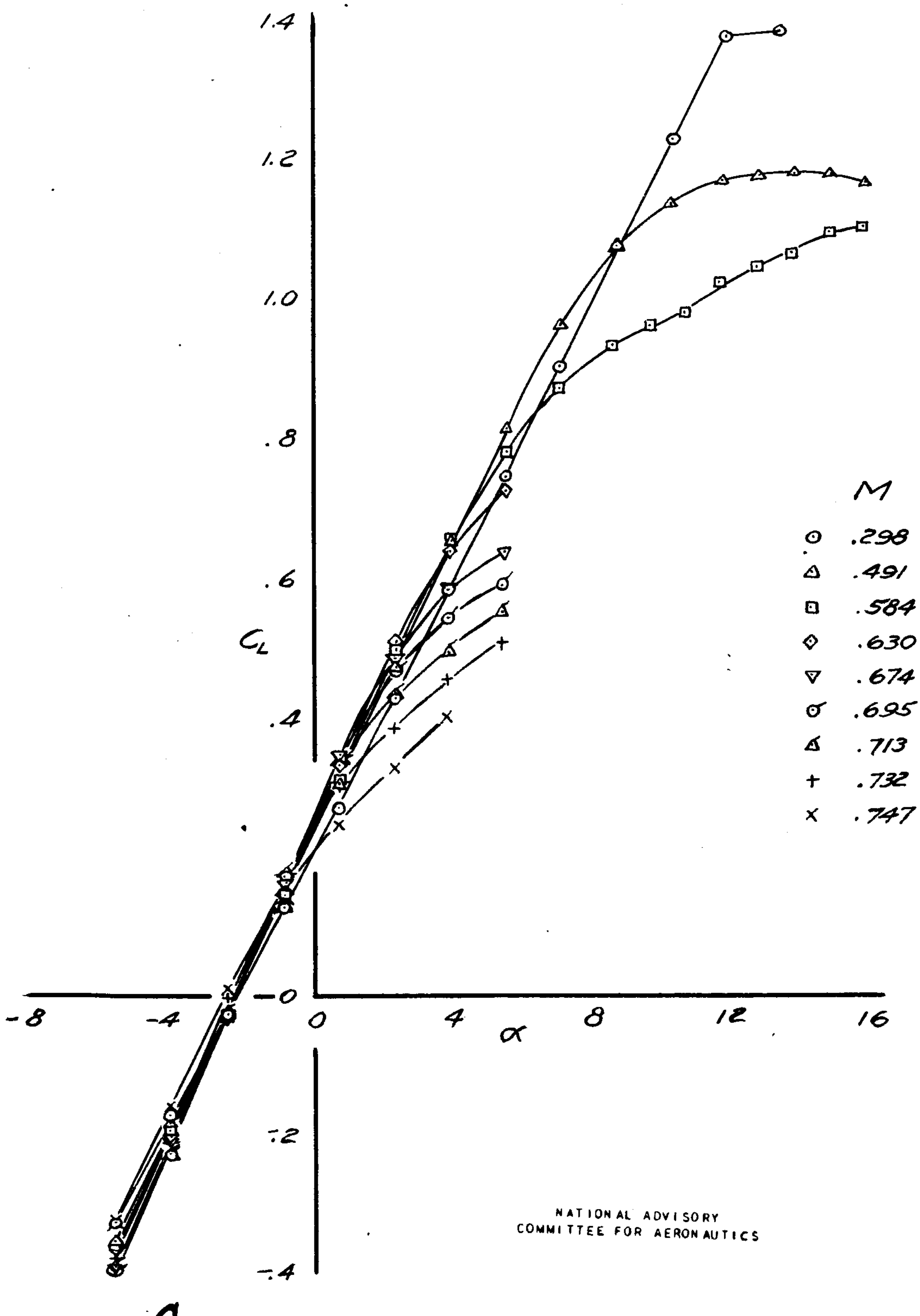

FIGURE 4(6) - LIFT CHARACTERISTICS OF THE MODEL WITH THE NACA 230-SERIES WING.

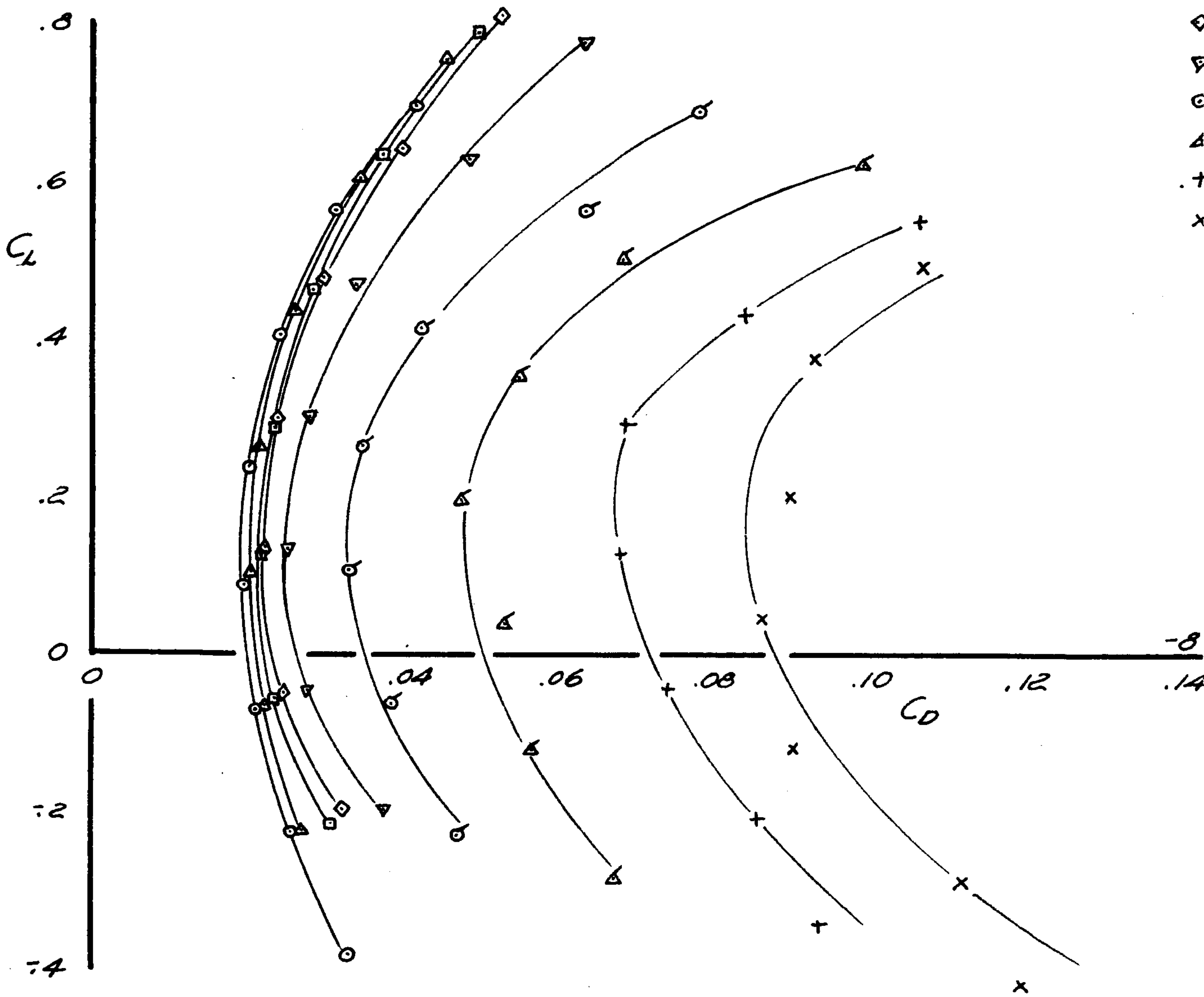

FIGURE 5A

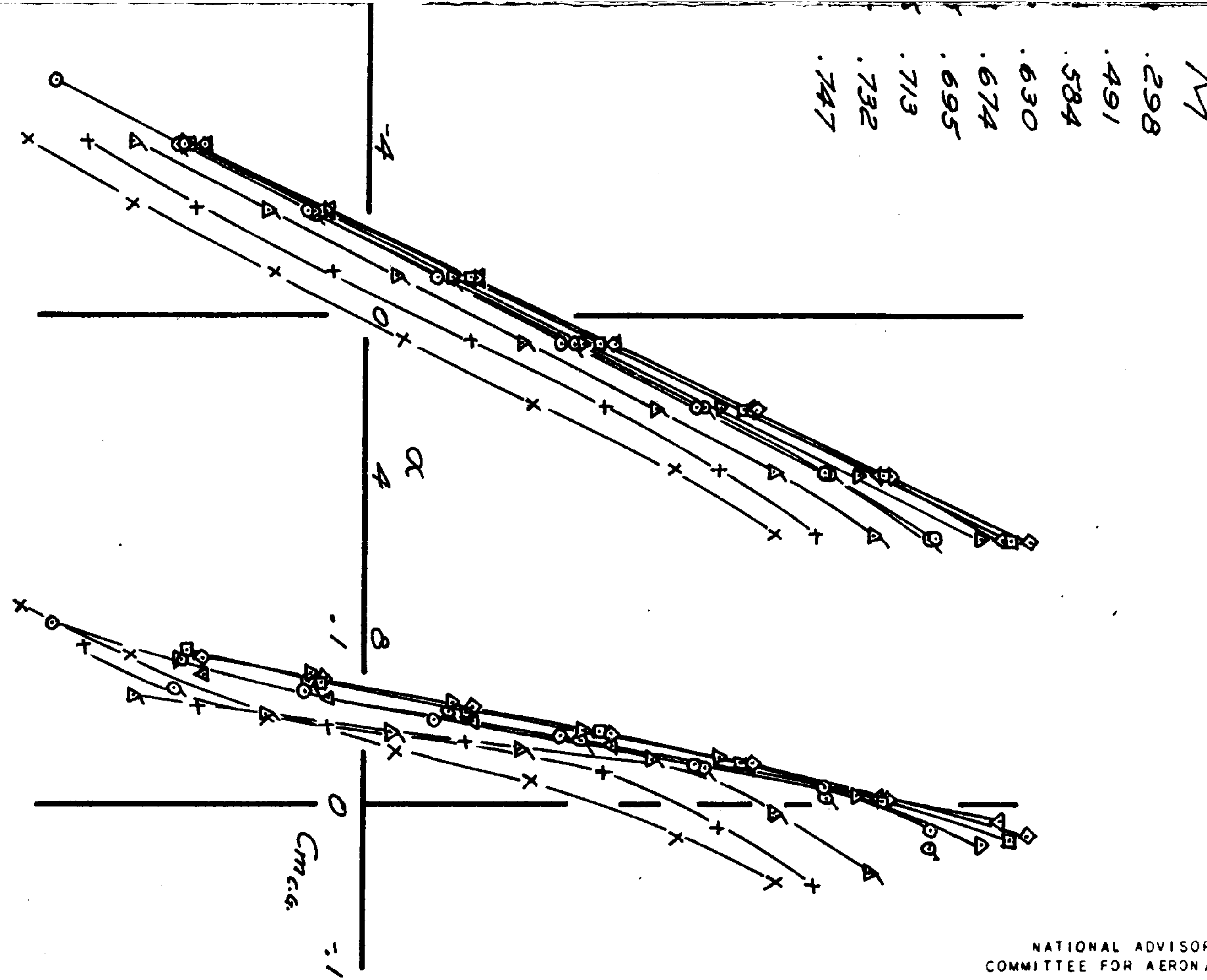

NATIONAL ADVISORY
COMMITTEE FOR AERONAUTICS

FIGURE 5B LIFT, DRAG, AND PITCHING-MOMENT CHARACTERISTICS OF THE MODEL WITH THE HIGHLY CAMBERED NACA 66-SERIES WING. STABILIZER ANGLE, 0°.

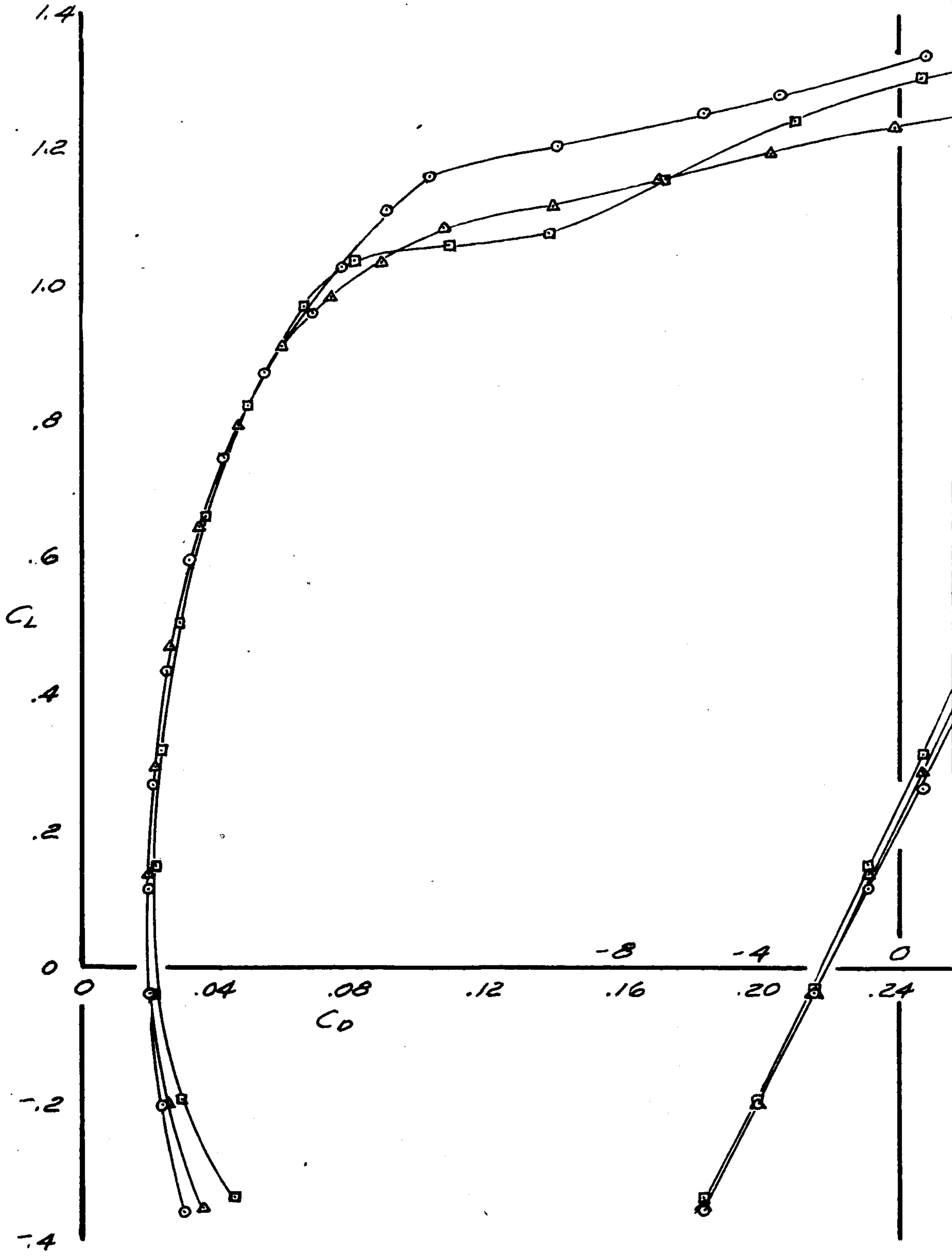

FIGURE 6A

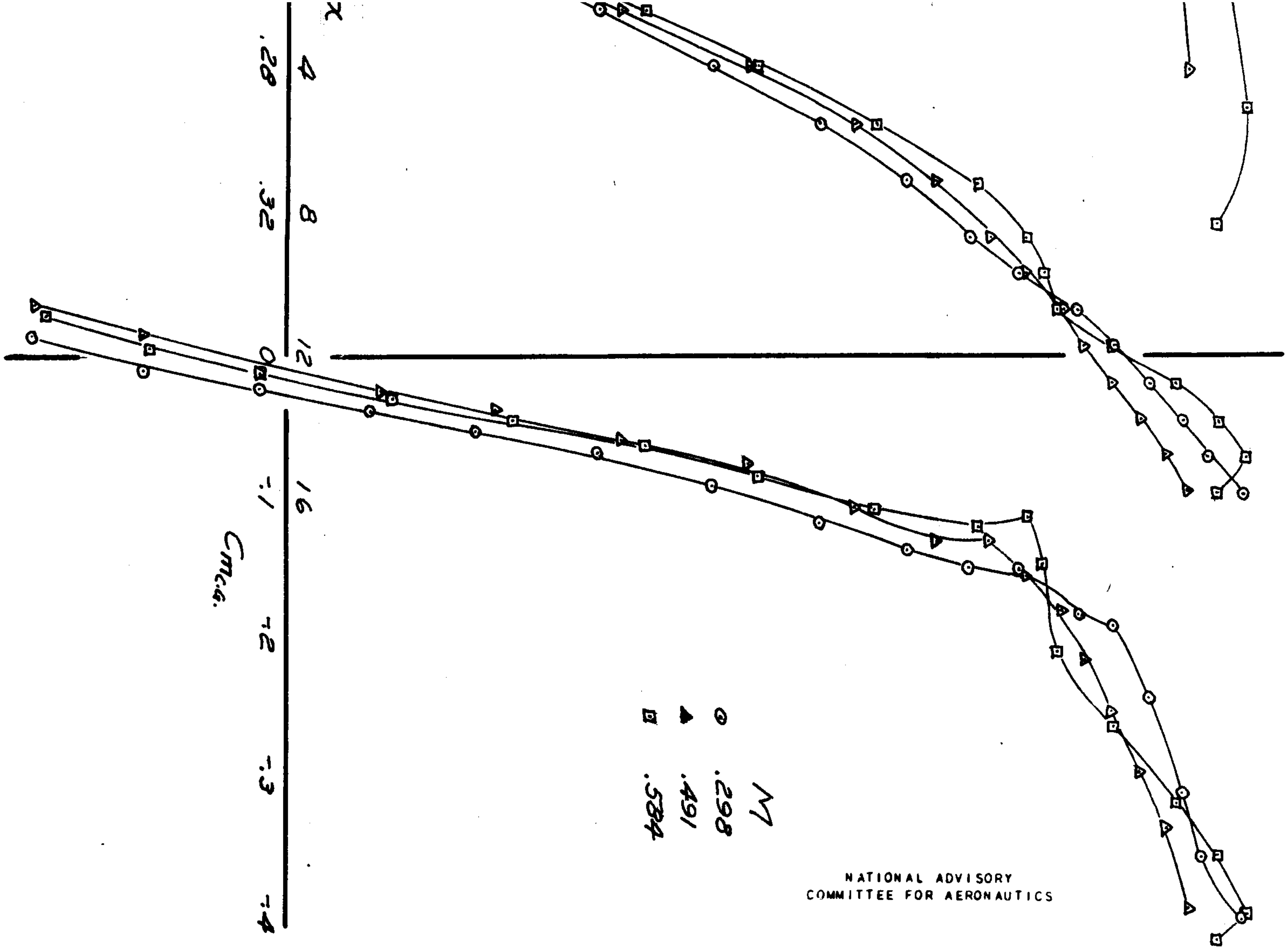

FIGURE 6B LIFT, DRAG, AND PITCHING-MOMENT CHARACTERISTICS OF THE MODEL WITH THE HIGHLY CAMBERED NACA 66-SERIES WING. STABILIZER ANGLE, +2°.

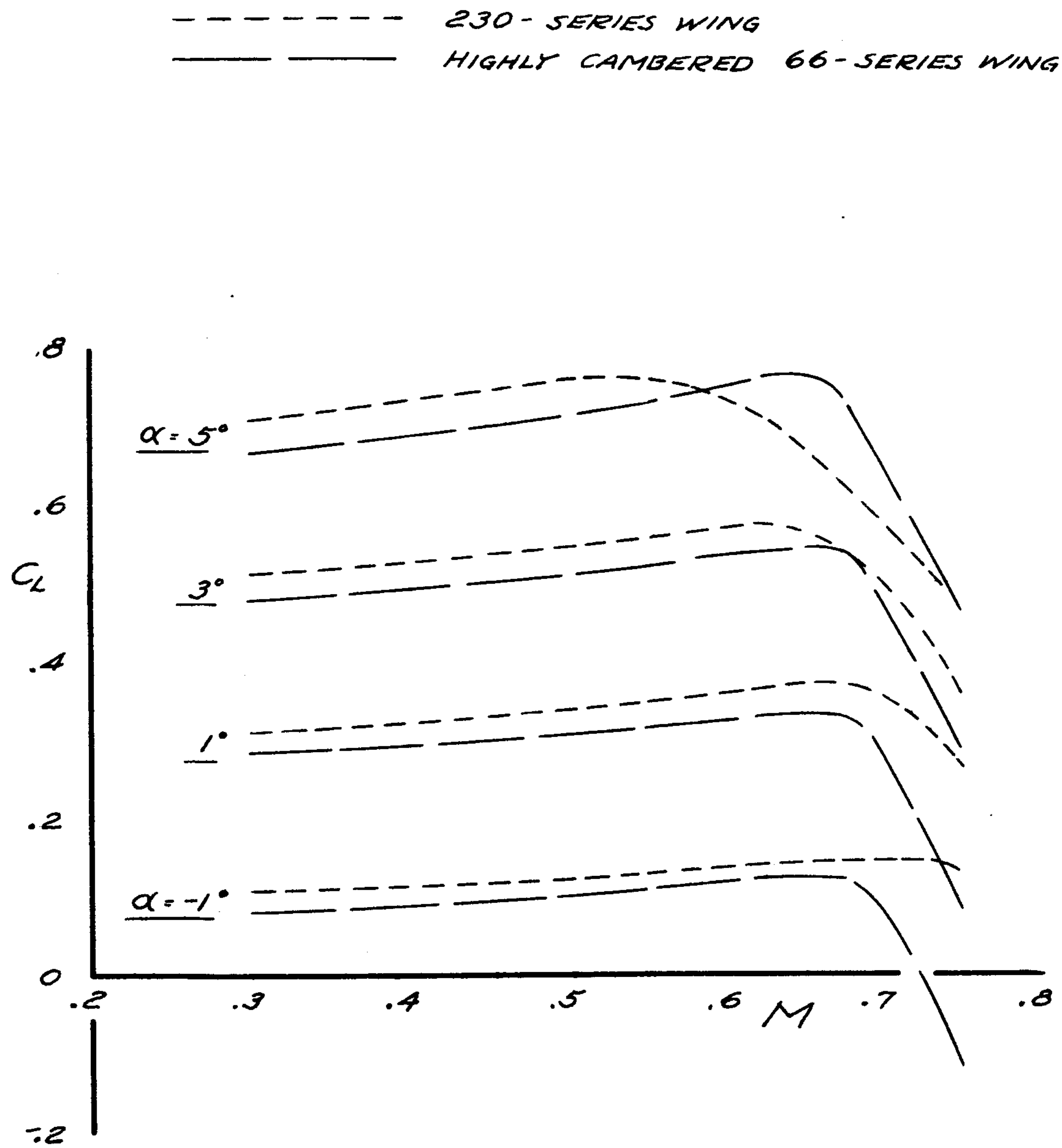

NATIONAL ADVISORY COMMITTEE FOR AERONAUTICS

FIGURE 7(a). - COMPARISON OF AERODYNAMIC CHARACTERISTICS OF THE MODEL WITH THE 230 - SERIES WING AND WITH THE HIGHLY CAMBERED 66 - SERIES WING. VARIATION OF LIFT COEFFICIENT WITH MACH NUMBER.

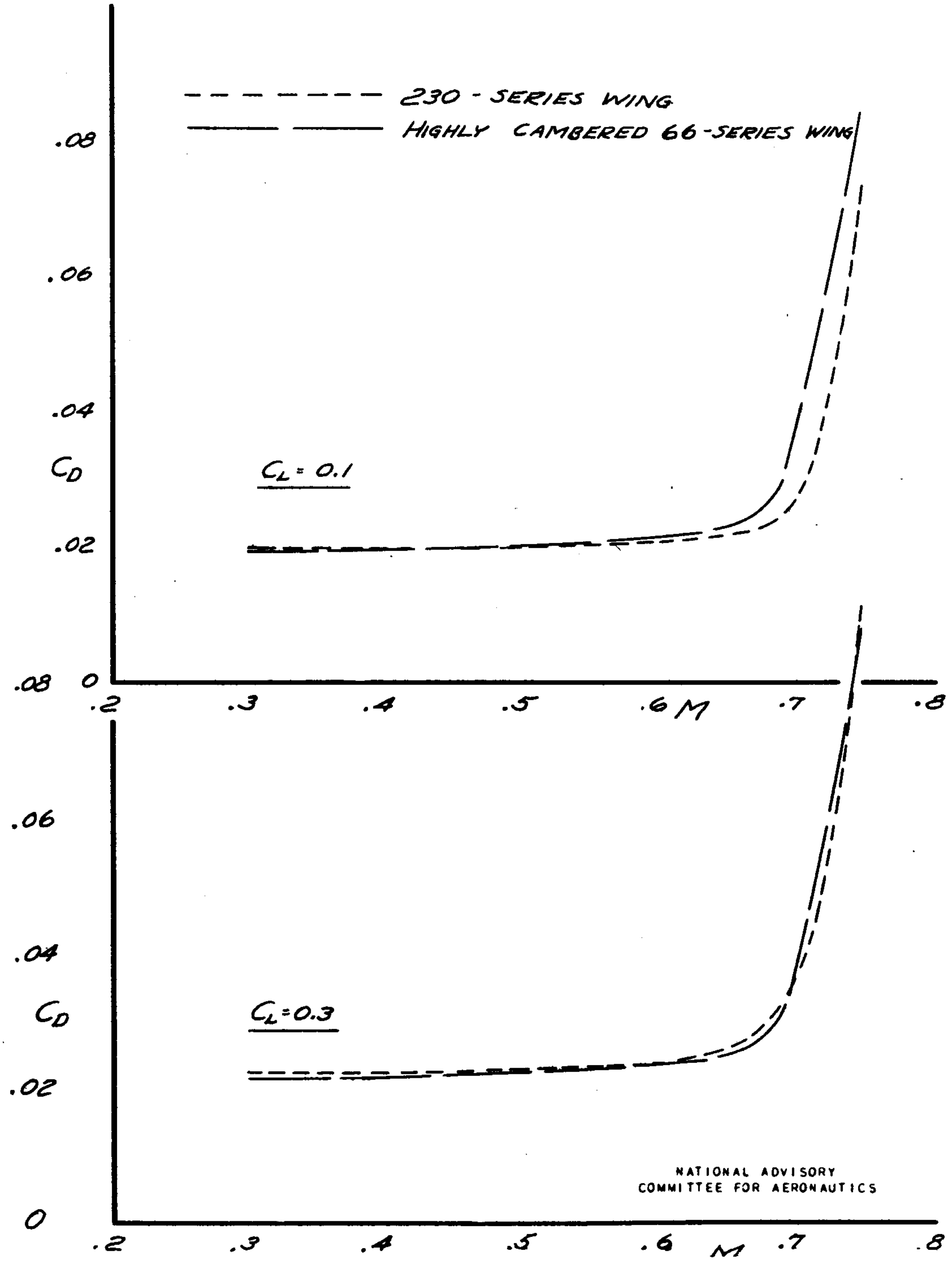

FIGURE 7(b).- COMPARISON OF AERODYNAMIC CHARACTERISTICS OF THE MODEL WITH THE 230-SERIES WING AND WITH THE HIGHLY CAMBERED 66-SERIES WING. VARIATION OF DRAG COEFFICIENT WITH MACH NUMBER AT LIFT COEFFICIENTS OF 0.1 AND 0.3.

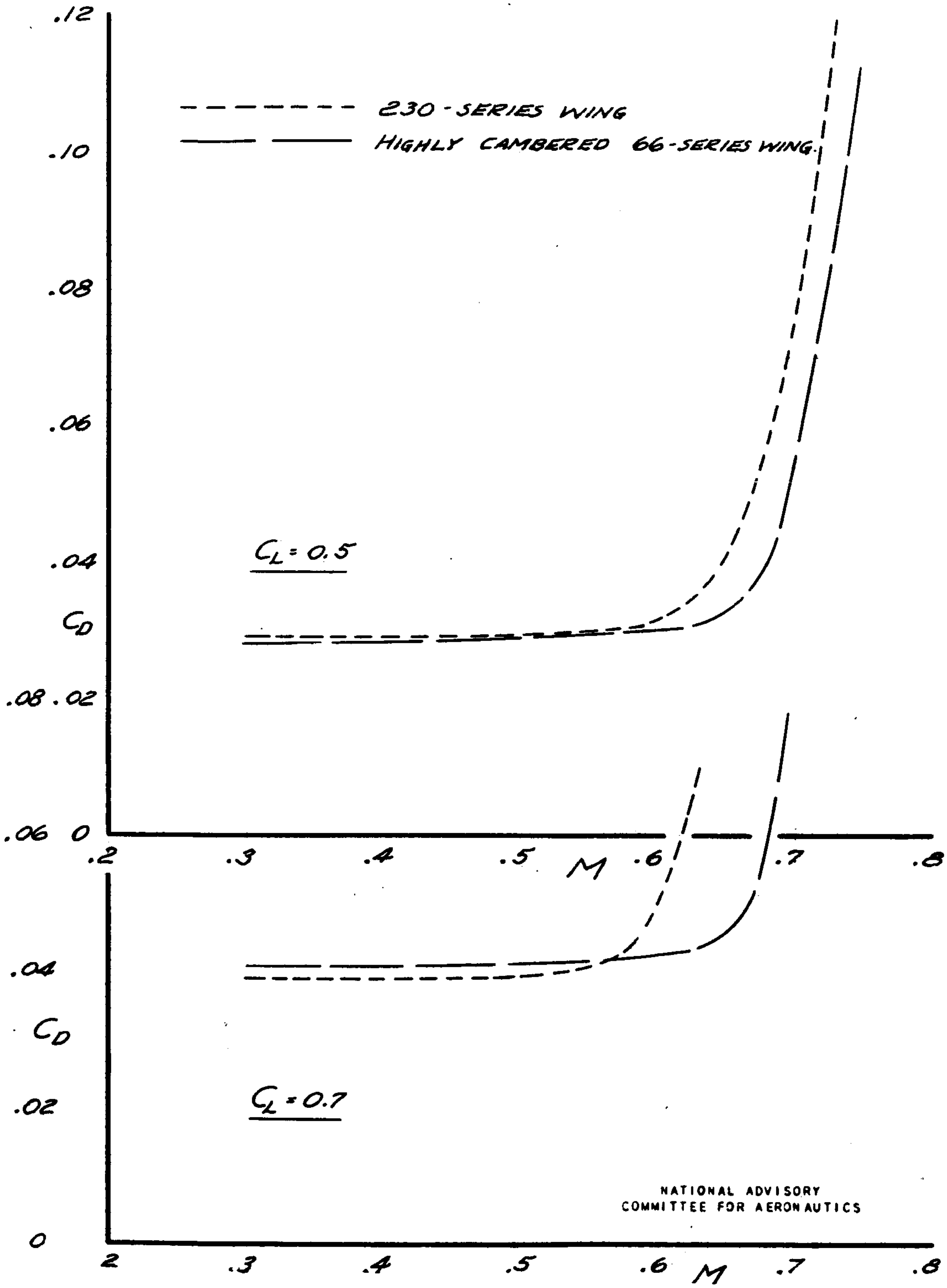

FIGURE 7(c).- COMPARISON OF AERODYNAMIC CHARACTERISTICS OF THE MODEL WITH THE 230-SERIES WING AND WITH THE HIGHLY CAMBERED 66-SERIES WING. VARIATION OF DRAG COEFFICIENT WITH MACH NUMBER AT LIFT COEFFICIENTS OF 0.5 AND 0.7.

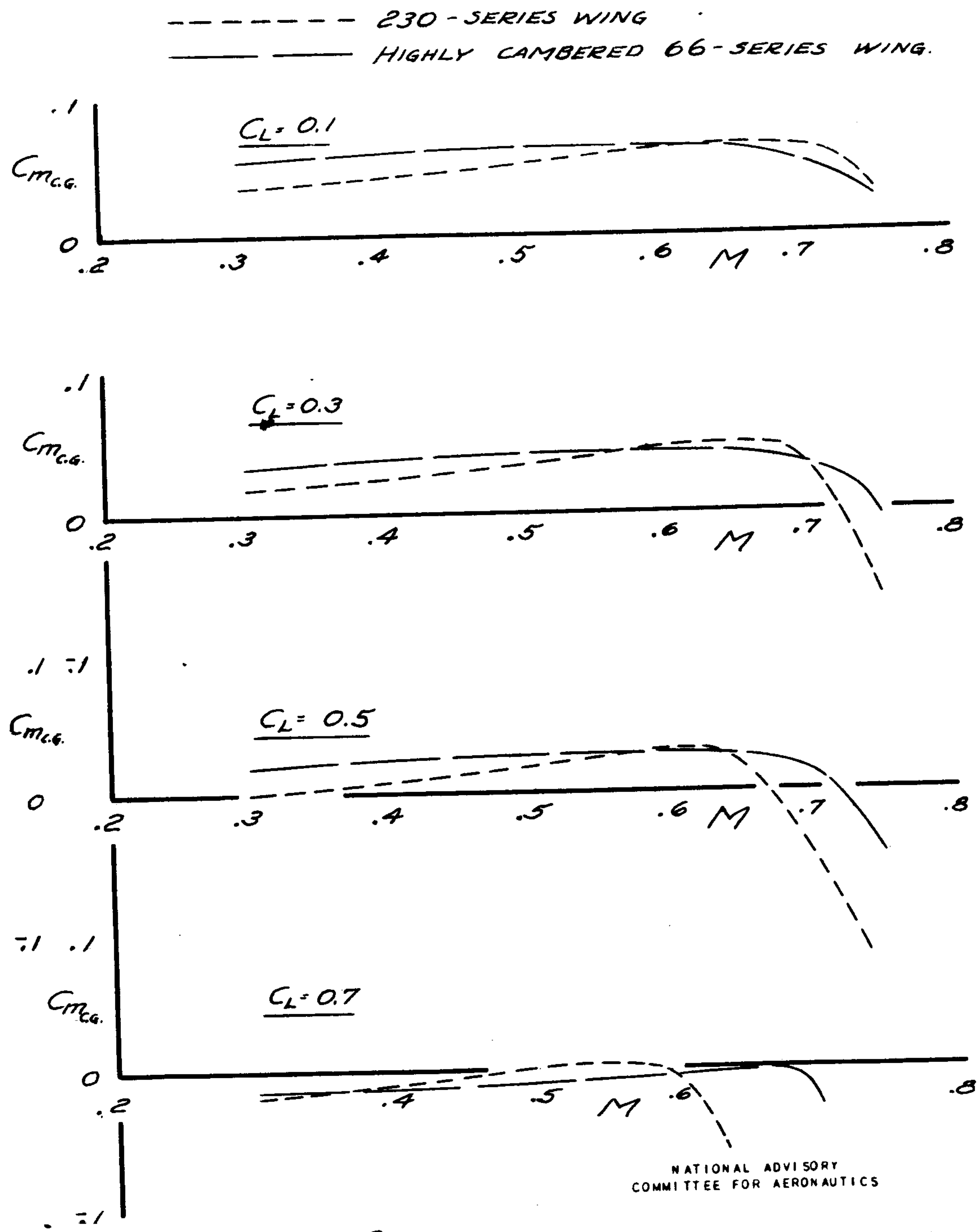

FIGURE 7(d).- COMPARISON OF AERODYNAMIC CHARACTERISTICS OF THE MODEL WITH THE 230 - SERIES WING AND WITH THE HIGHLY CAMBERED 66 - SERIES WING. VARIATION OF PITCHING - MOMENT COEFFICIENT WITH MACH NUMBER.

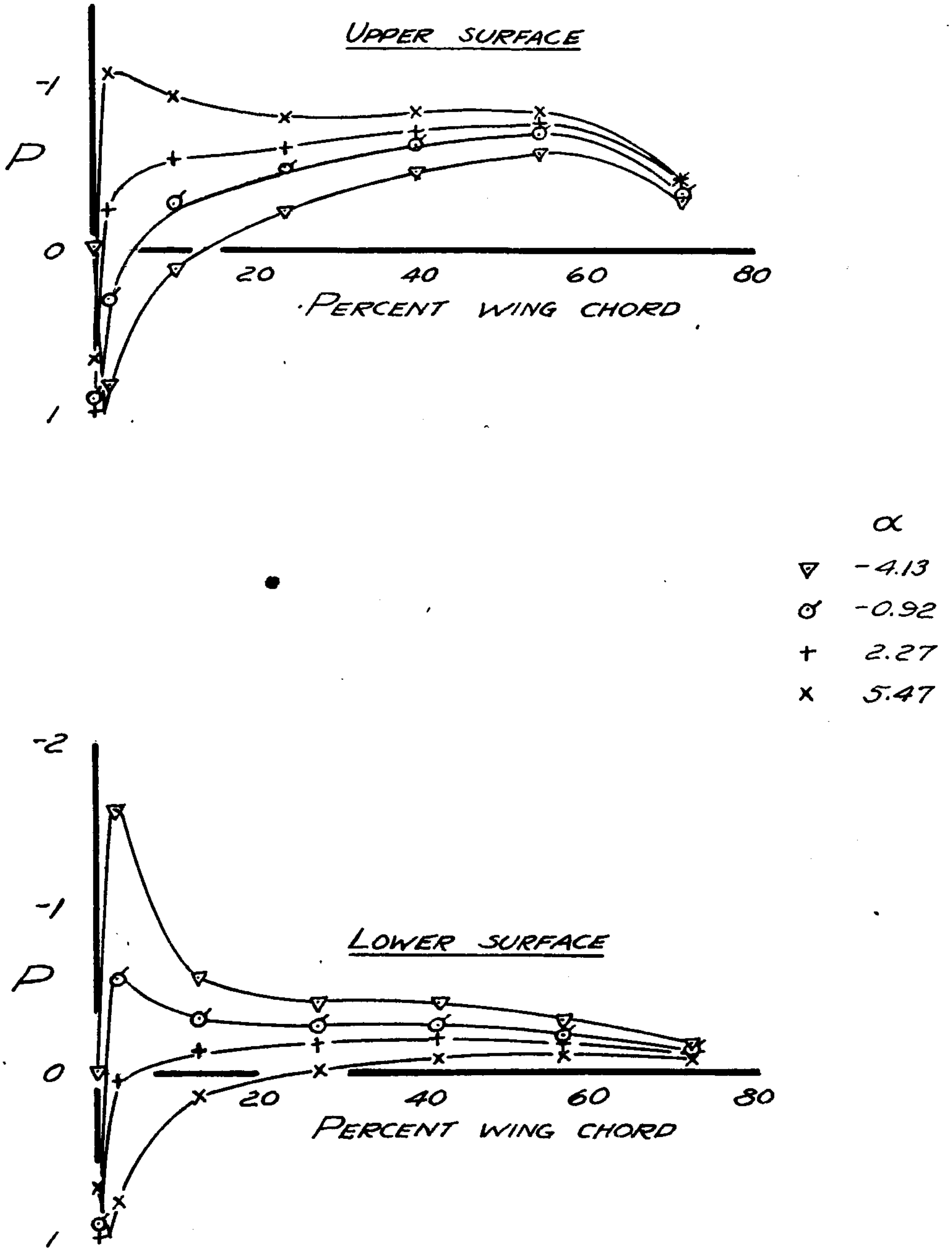

NATIONAL ADVISORY
COMMITTEE FOR AERONAUTICS

FIGURE 8(a). - PRESSURE DISTRIBUTION AT WING STATION 28.6 ON THE HIGHLY CAMBERED 66-SERIES WING. MACH NUMBER, 0.298.

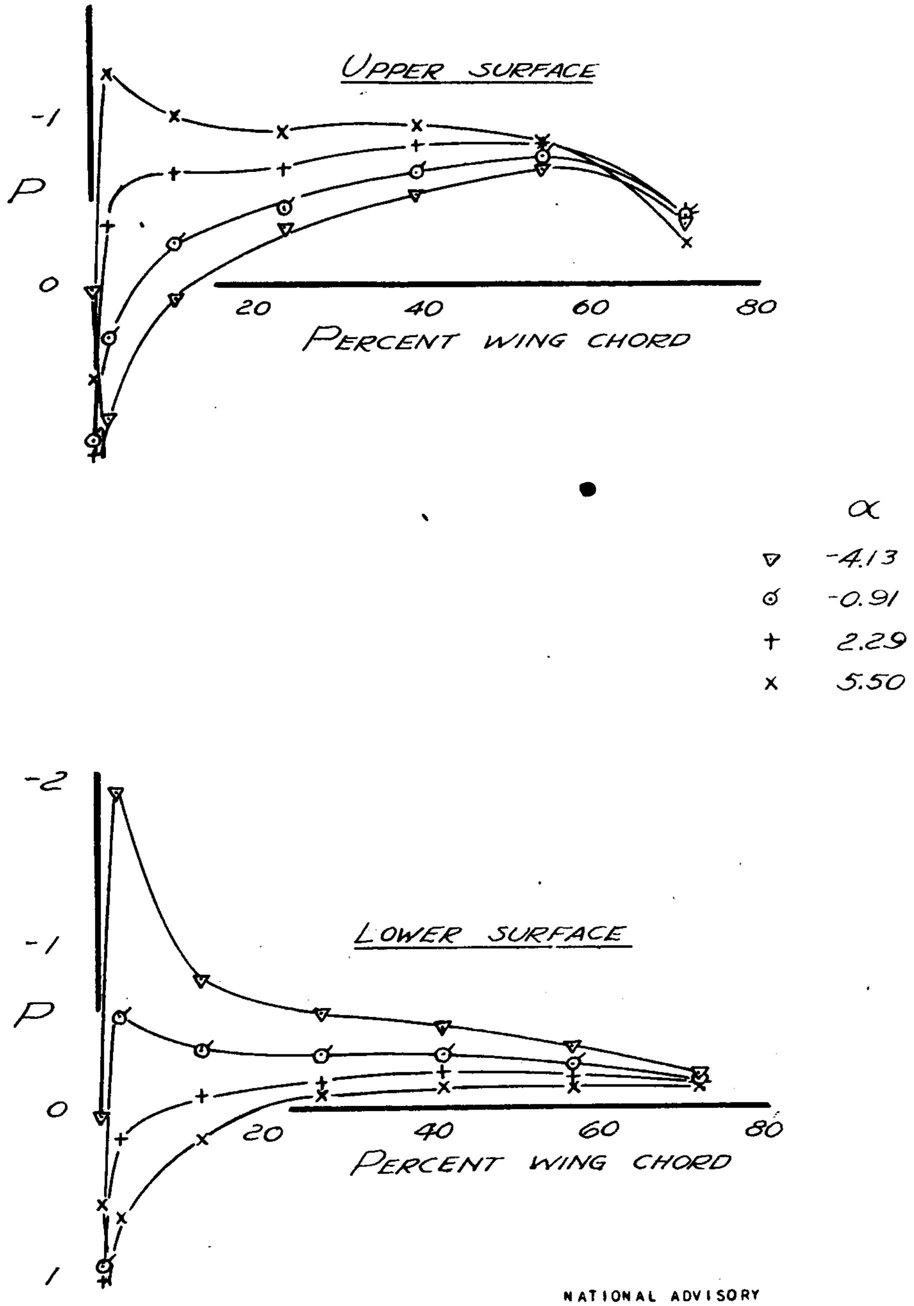

NATIONAL ADVISORY
COMMITTEE FOR AERONAUTICS

FIGURE 8(b). - PRESSURE DISTRIBUTION AT WING STATION 28.6 ON THE HIGHLY CAMBERED 66-SERIES WING. MACH NUMBER, 0.491.

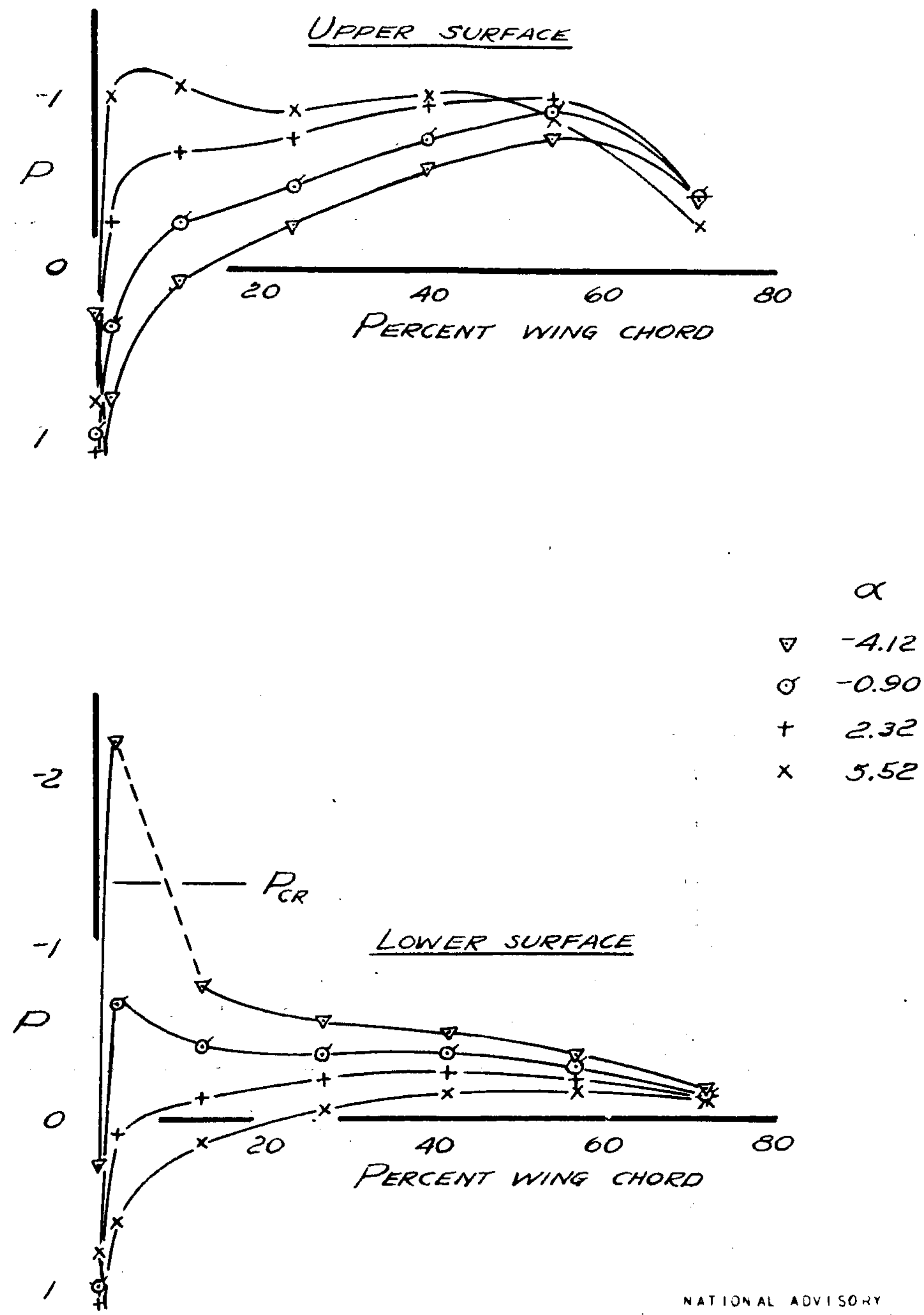

NATIONAL ADVISORY COMMITTEE FOR AERONAUTICS

FIGURE 8(c).- PRESSURE DISTRIBUTION AT WING STATION 28.6 ON THE HIGHLY CAMBERED 66-SERIES WING. MACH NUMBER, 0.584.

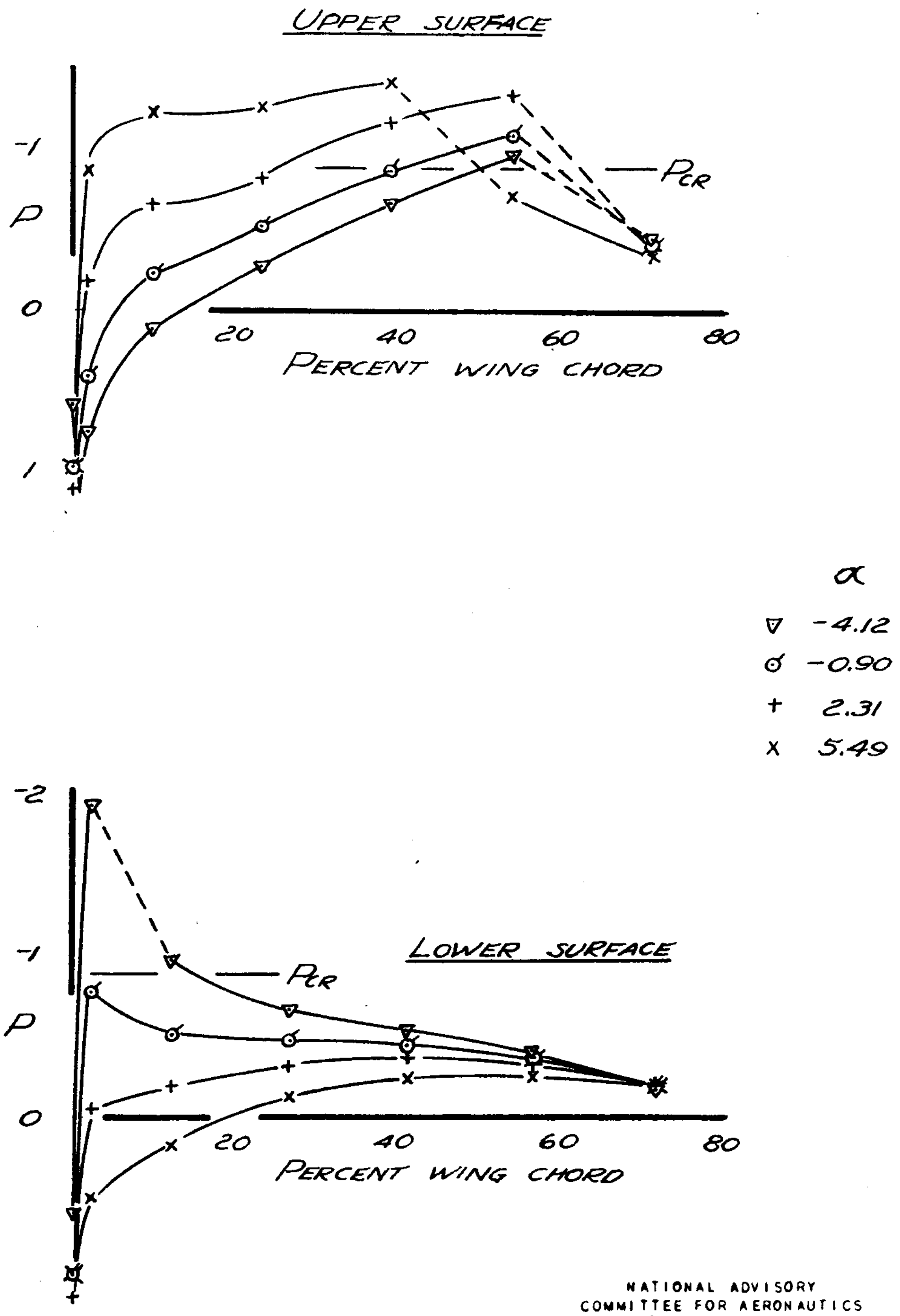

NATIONAL ADVISORY COMMITTEE FOR AERONAUTICS

FIGURE 8(d).- PRESSURE DISTRIBUTION AT WING STATION 28.6 ON THE HIGHLY CAMBERED 66-SERIES WING. MACH NUMBER, 0.674.

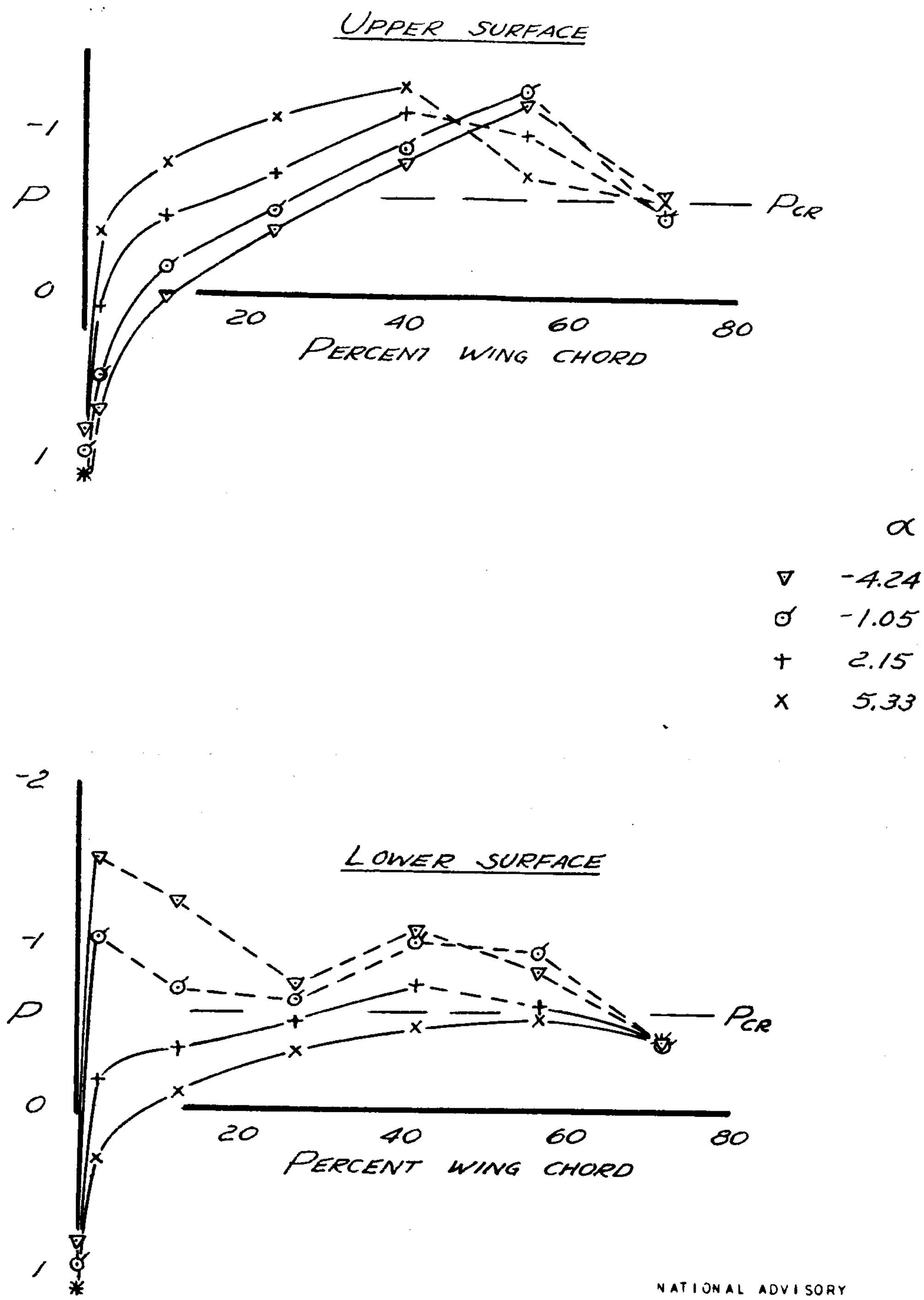

NATIONAL ADVISORY
COMMITTEE FOR AERONAUTICS

FIGURE 8(e). - PRESSURE DISTRIBUTION AT WING STATION 28.6 ON THE HIGHLY CAMBERED 66-SERIES WING. MACH NUMBER, 0.747.

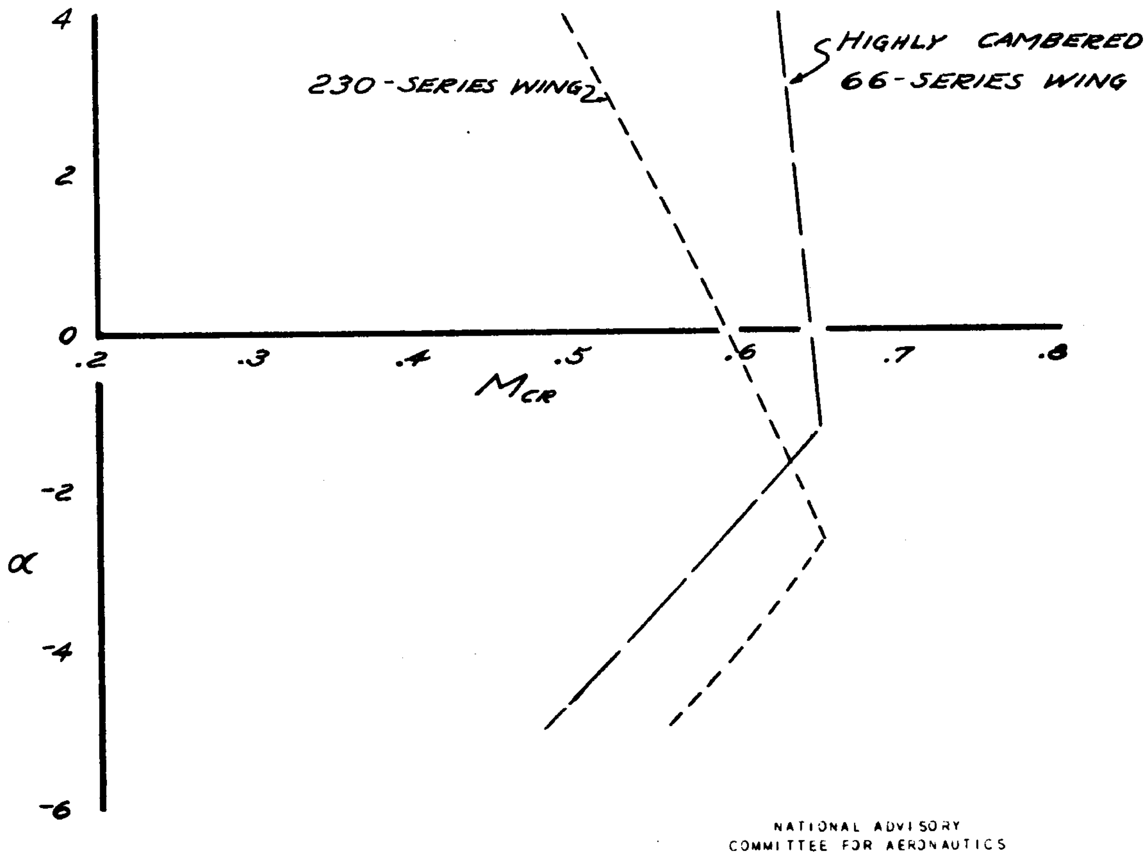

FIGURE 9. - CRITICAL MACH NUMBER OF THE 230 - SERIES WING AND THE HIGHLY CAMBERED 66 - SERIES WING.

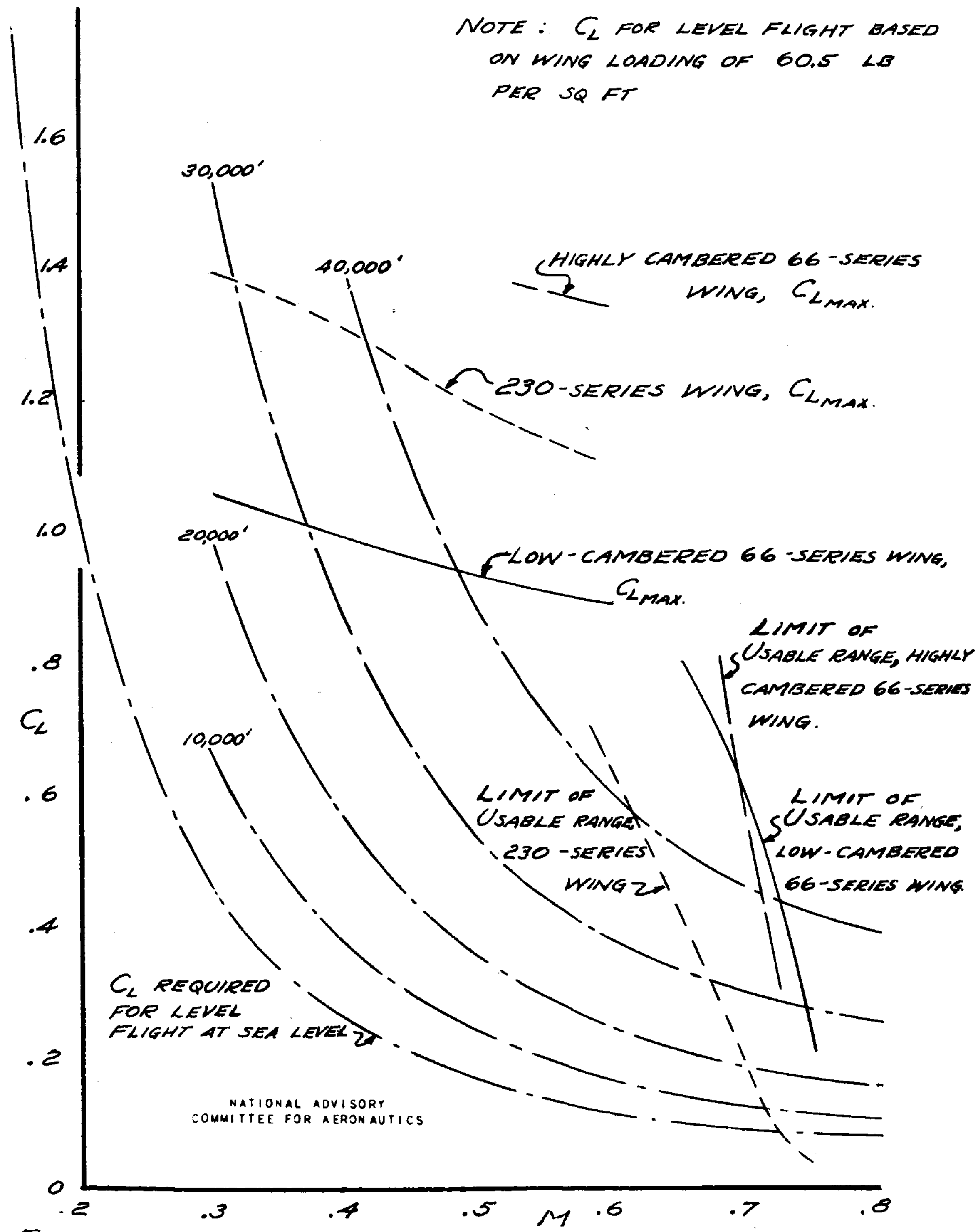

FIGURE 10.- MAXIMUM LIFT COEFFICIENT, USABLE MACH NUMBER RANGE, AND LIFT COEFFICIENT FOR LEVEL FLIGHT WITH THE 230-SERIES WING, THE HIGHLY CAMBERED 66-SERIES WING, AND THE LOW-CAMBERED 66-SERIES WING.

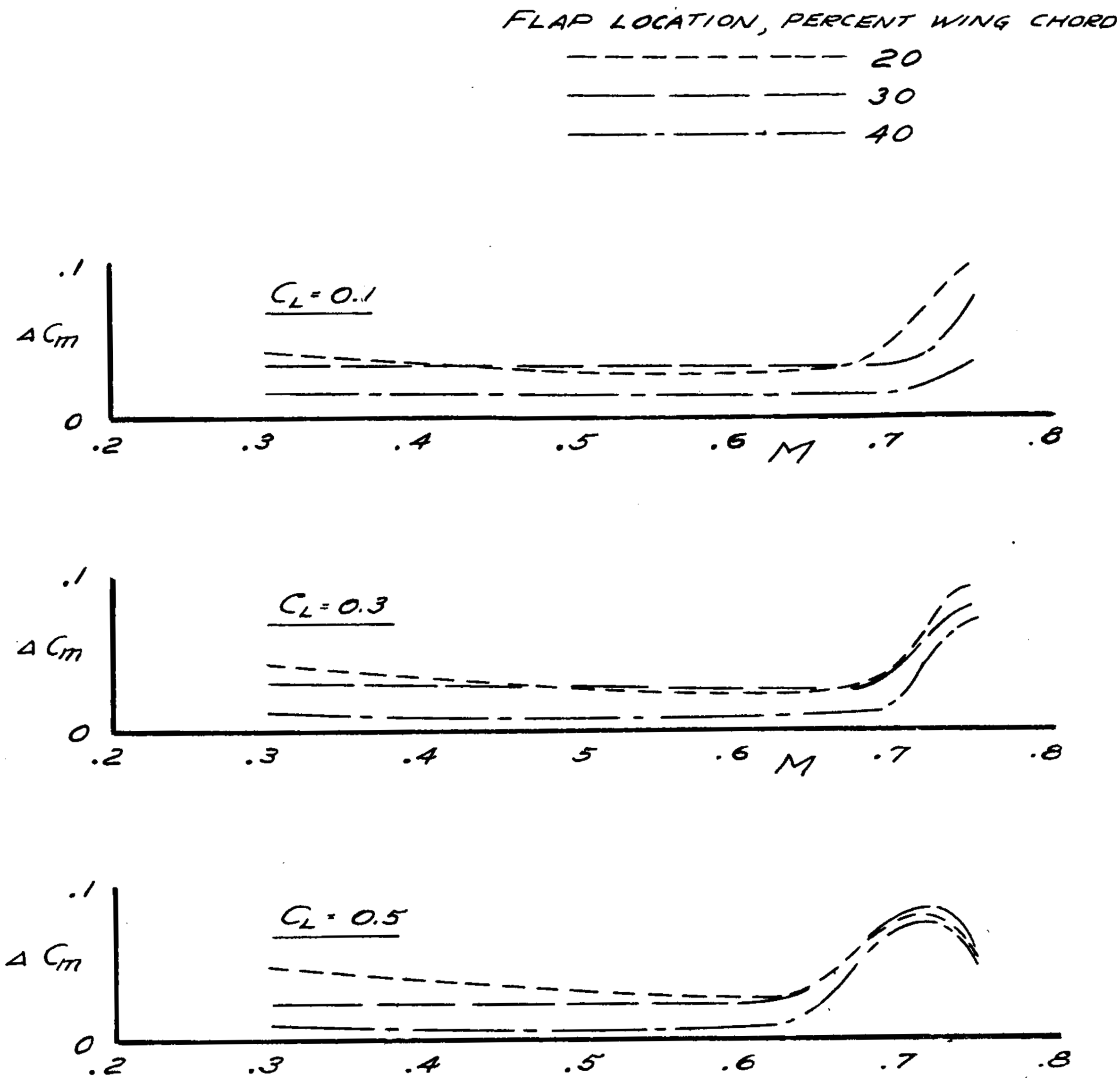

NATIONAL ADVISORY
COMMITTEE FOR AERONAUTICS

FIGURE 11.- ADDITIONAL PITCHING-MOMENT COEFFICIENT FROM THE OUTBOARD 45° AUXILIARY CONTROL FLAPS AT VARIOUS CHORDWISE LOCATIONS ON THE 230-SERIES WING.

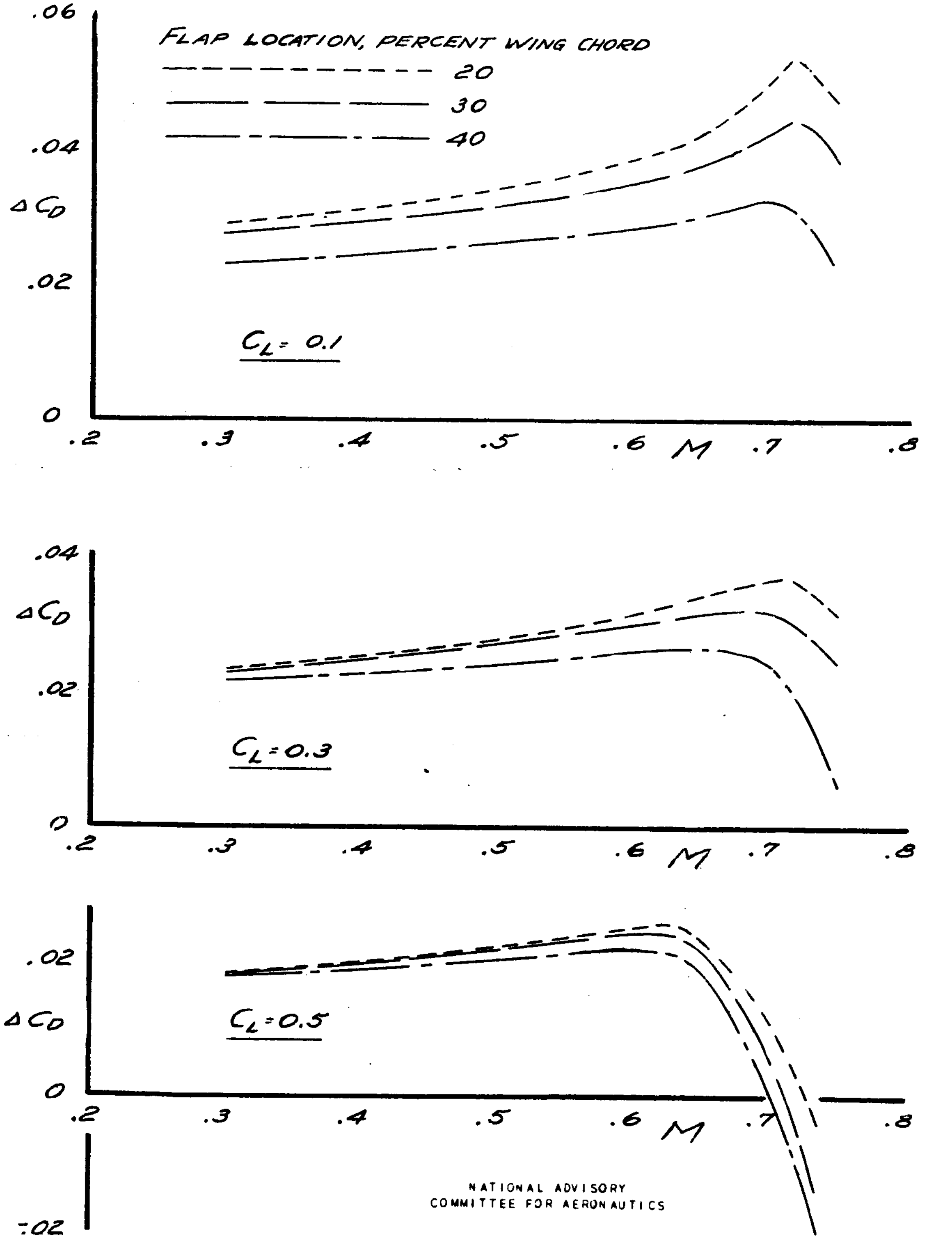

FIGURE 12.- ADDITIONAL DRAG COEFFICIENT FROM THE OUTBOARD 45° AUXILIARY CONTROL FLAPS AT VARIOUS CHORDWISE LOCATIONS ON THE 230-SERIES WING.

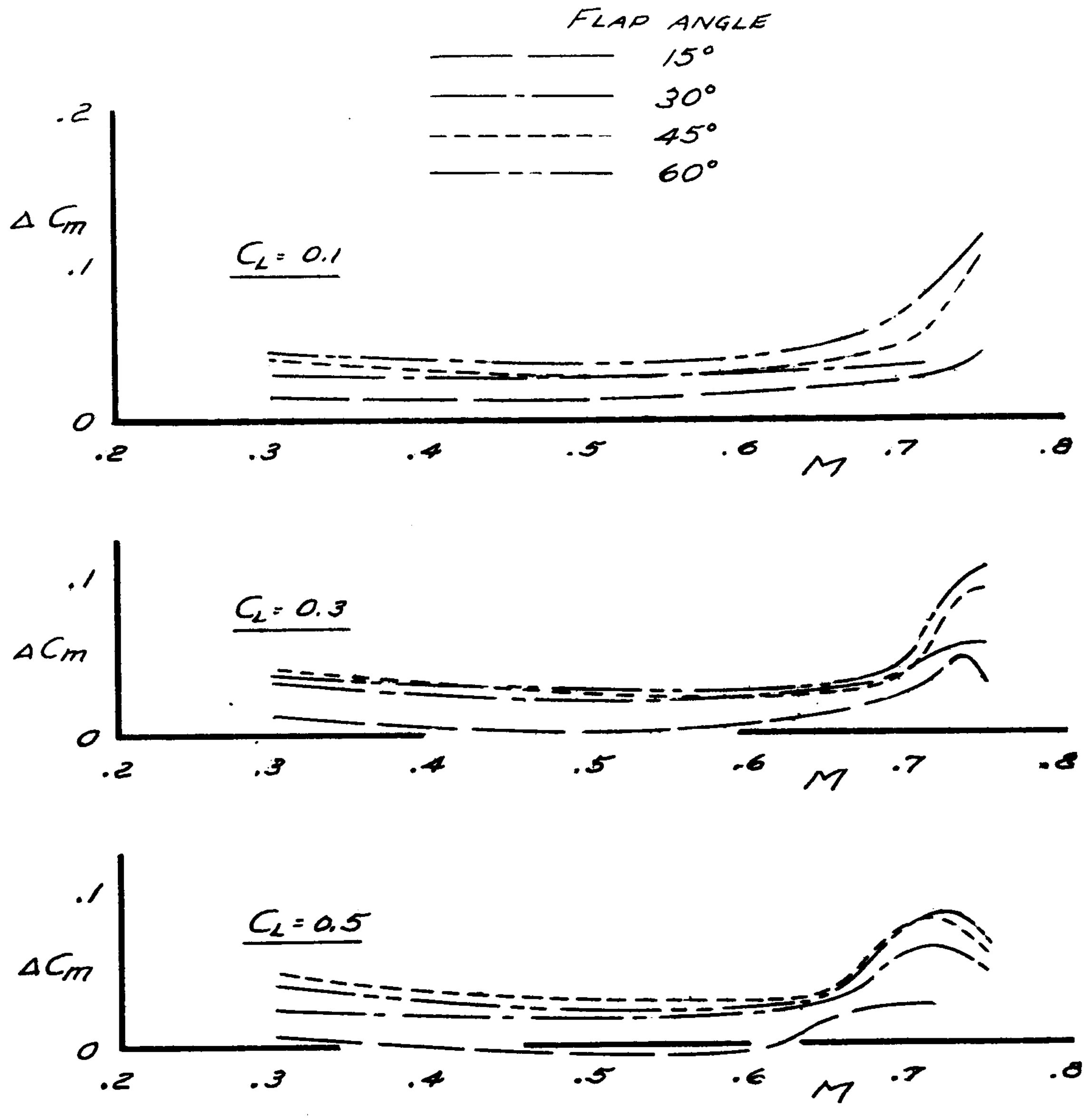

NATIONAL ADVISORY
COMMITTEE FOR AERONAUTICS

FIGURE 13.- ADDITIONAL PITCHING-MOMENT COEFFICIENT FROM VARIOUS DEFLECTIONS OF THE OUTBOARD AUXILIARY CONTROL FLAPS AT 20-PERCENT WING CHORD ON THE 230-SERIES WING.

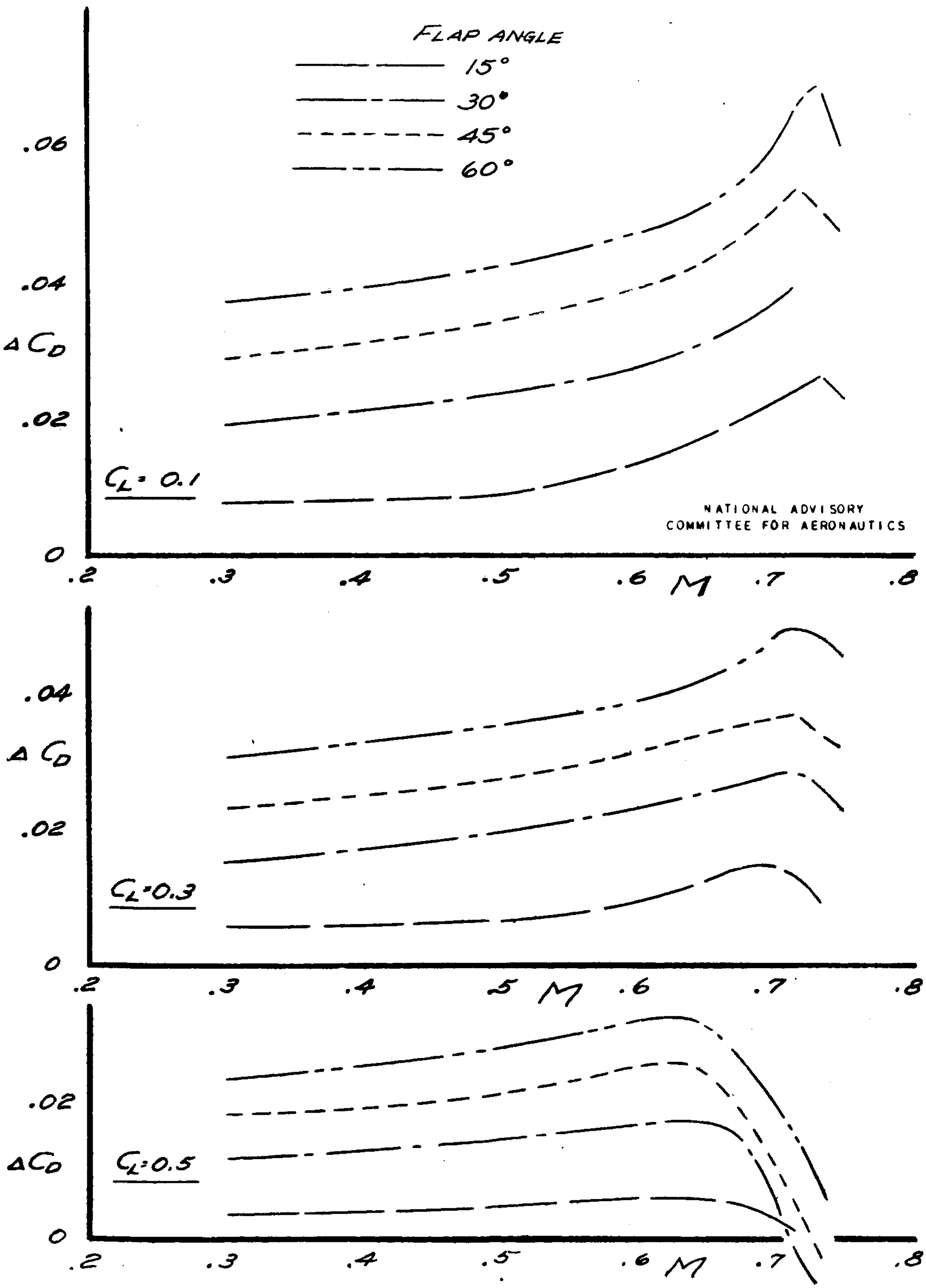

FIGURE 14.- ADDITIONAL DRAG COEFFICIENT FROM VARIOUS DEFLECTIONS OF THE OUTBOARD AUXILIARY CONTROL FLAPS AT 20-PERCENT WING CHORD ON THE 230-SERIES WING.

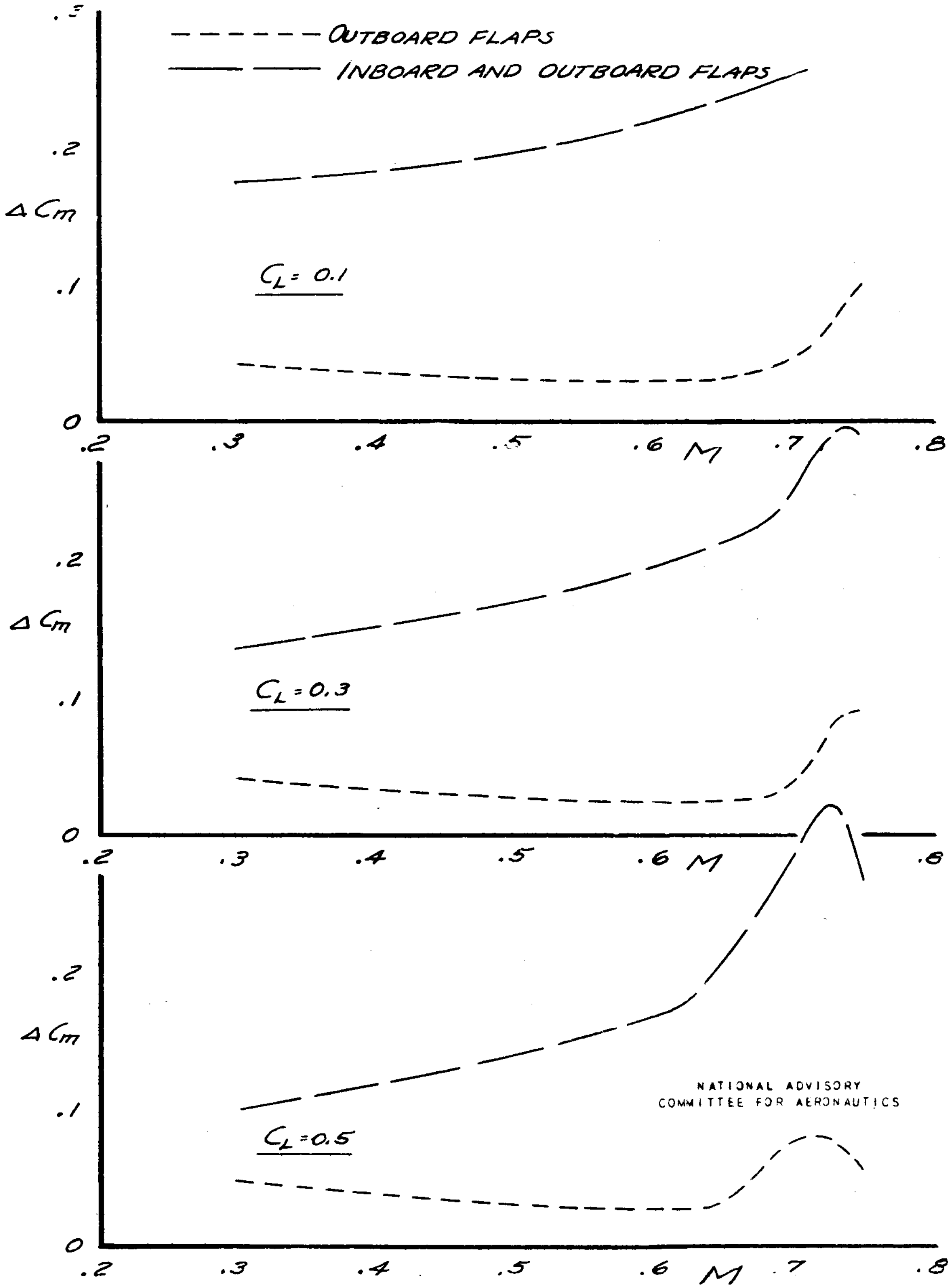

FIGURE 15.- ADDITIONAL PITCHING-MOMENT COEFFICIENT FROM OUTBOARD AND FROM INBOARD AND OUTBOARD 45° AUXILIARY CONTROL FLAPS AT 20-PERCENT WING CHORD ON THE 230-SERIES WING.

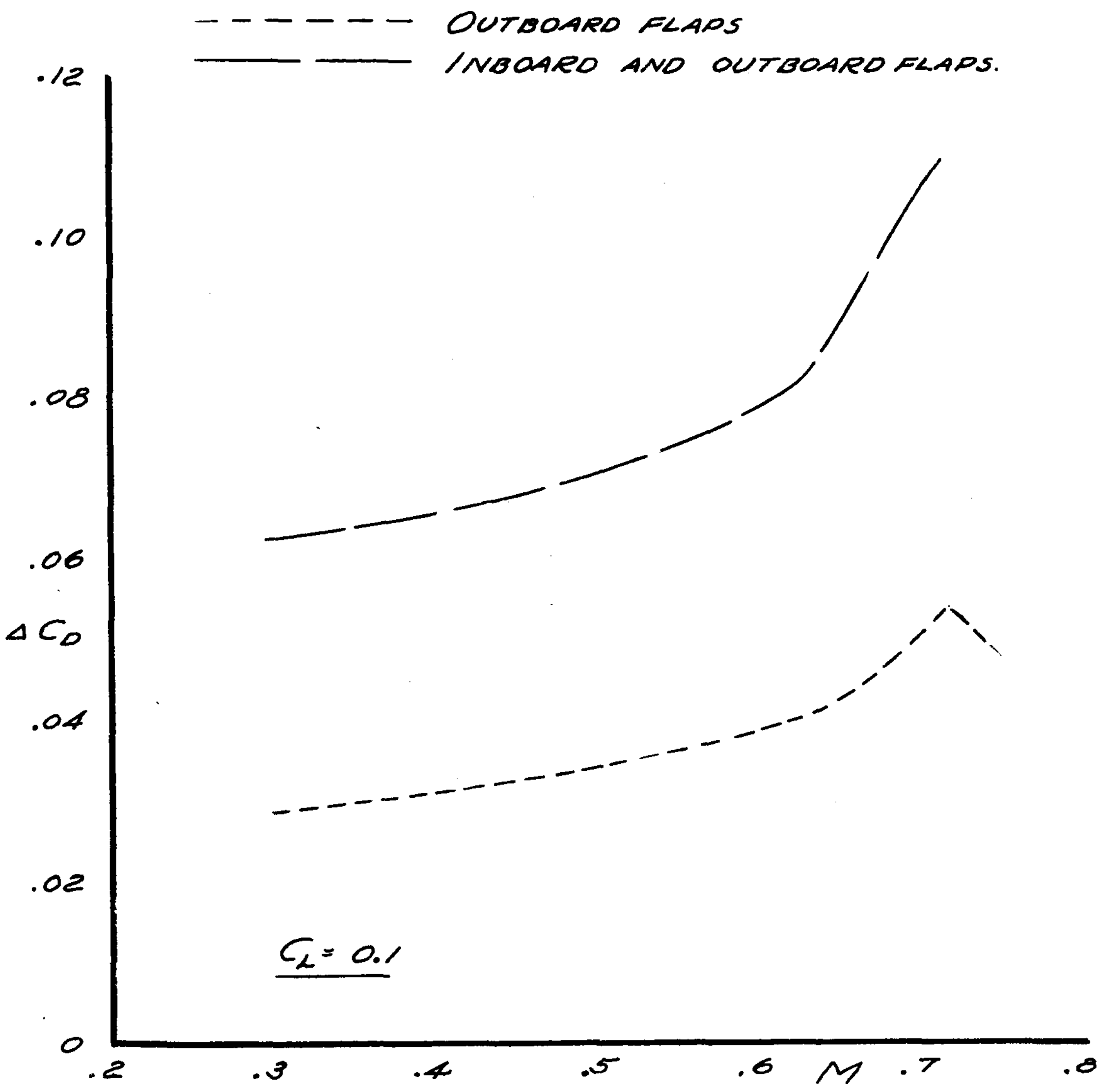

NATIONAL ADVISORY
COMMITTEE FOR AERONAUTICS

FIGURE 16(a).- ADDITIONAL DRAG COEFFICIENT FROM OUTBOARD AND FROM INBOARD AND OUTBOARD 45° AUXILIARY CONTROL FLAPS AT 20-PERCENT WING CHORD ON THE 230-SERIES WING. LIFT COEFFICIENT, 0.1.

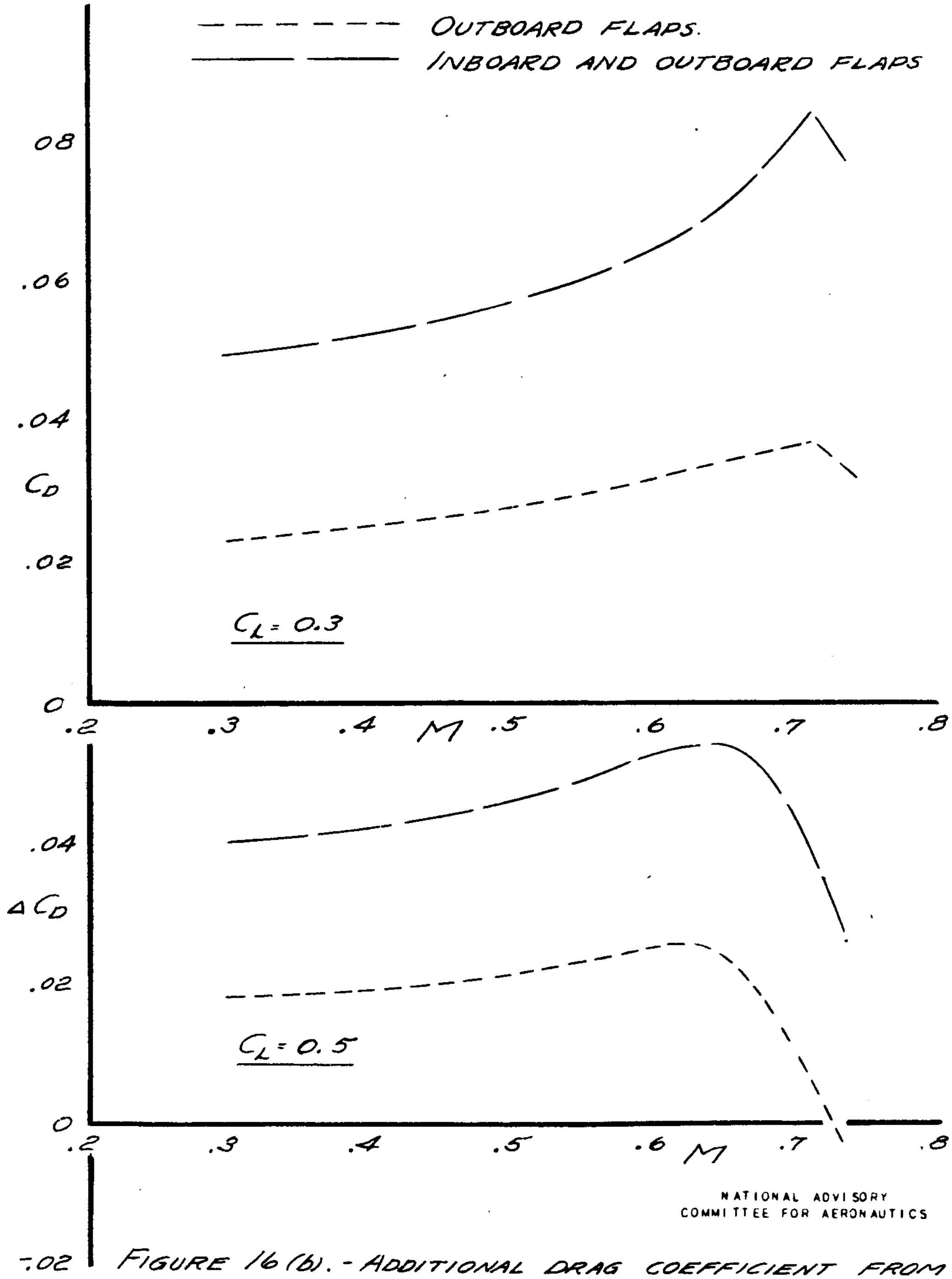

NATIONAL ADVISORY
COMMITTEE FOR AERONAUTICS

FIGURE 16 (b). - ADDITIONAL DRAG COEFFICIENT FROM OUTBOARD AND FROM INBOARD AND OUTBOARD 45° AUXILIARY CONTROL FLAPS AT 20-PERCENT WING CHORD ON THE 230-SERIES WING. LIFT COEFFICIENTS, 0.3 AND 0.5.

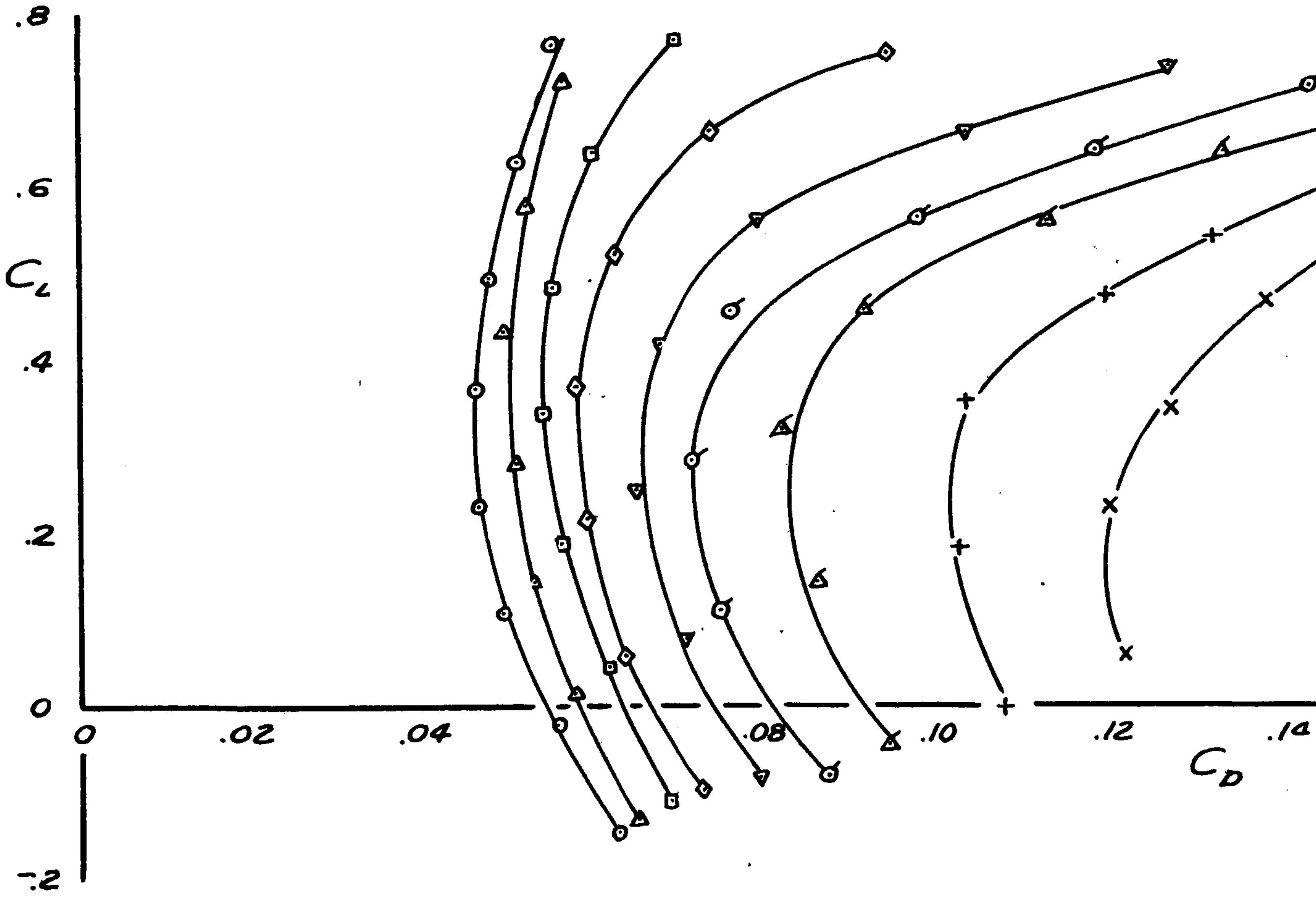

FIGURE 17A

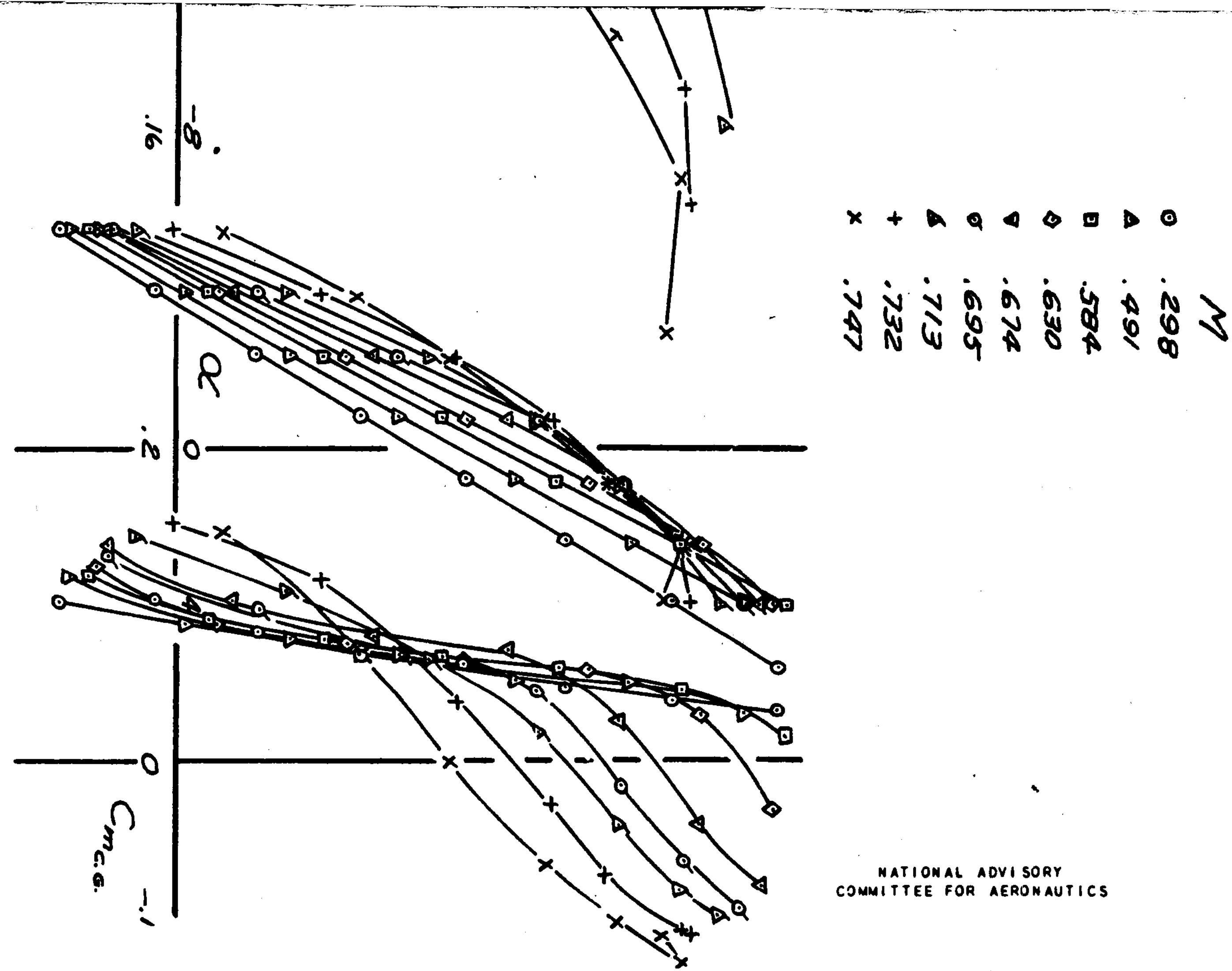

NATIONAL ADVISORY COMMITTEE FOR AERONAUTICS

FIGURE 17B LIFT, DRAG, AND PITCHING-MOMENT CHARACTERISTICS OF THE MODEL WITH THE NACA 230-SERIES WING AND OUTBOARD 45° AUXILIARY CONTROL FLAPS AT 20-PERCENT WING CHORD.

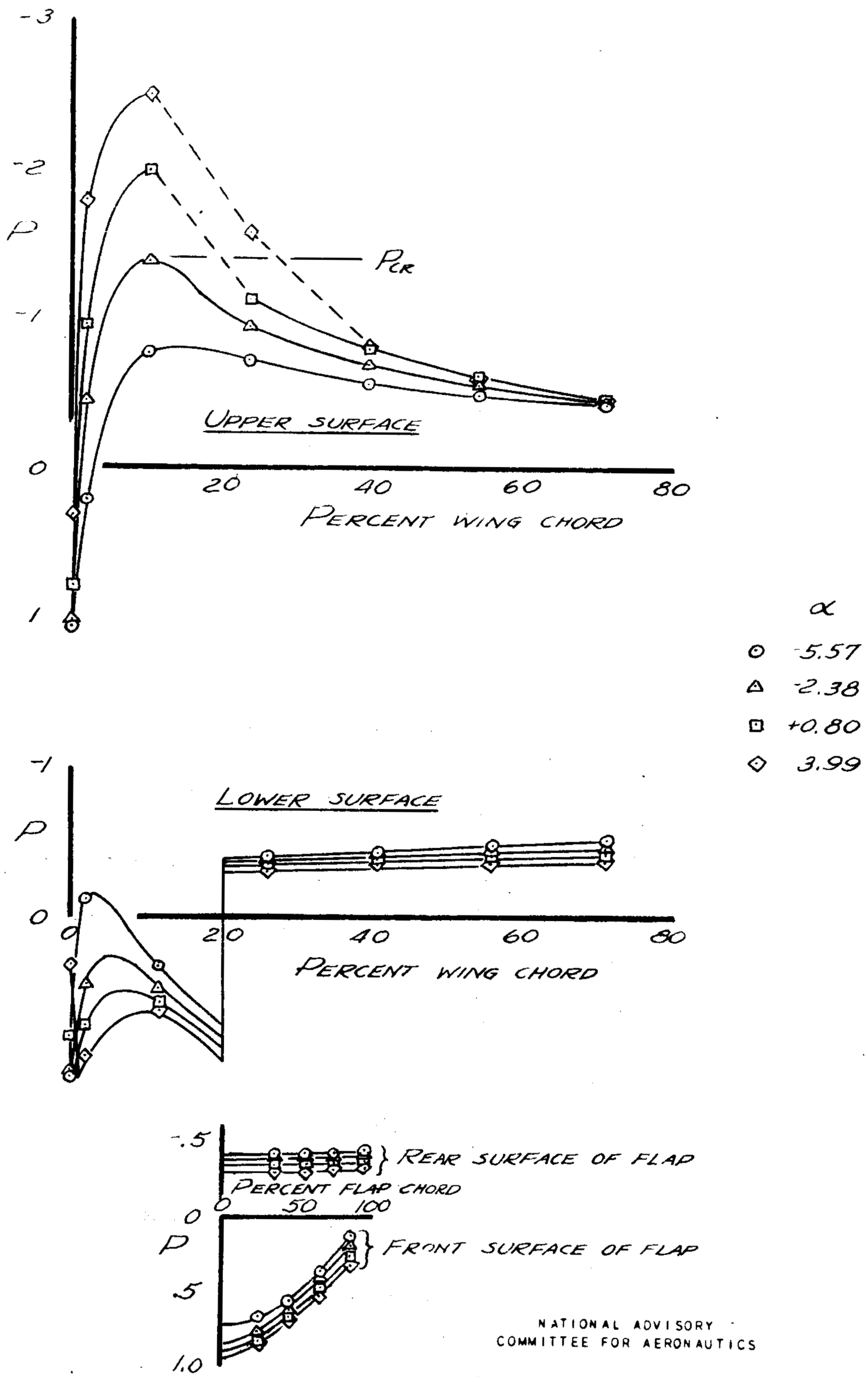

NATIONAL ADVISORY
COMMITTEE FOR AERONAUTICS

FIGURE 18(a).- WING AND FLAP PRESSURE DISTRIBUTION AT WING STATION 28.85 ON THE 230-SERIES WING WITH OUTBOARD 45° AUXILIARY CONTROL FLAPS AT 20-PERCENT WING CHORD. MACH NUMBER, 0.584.

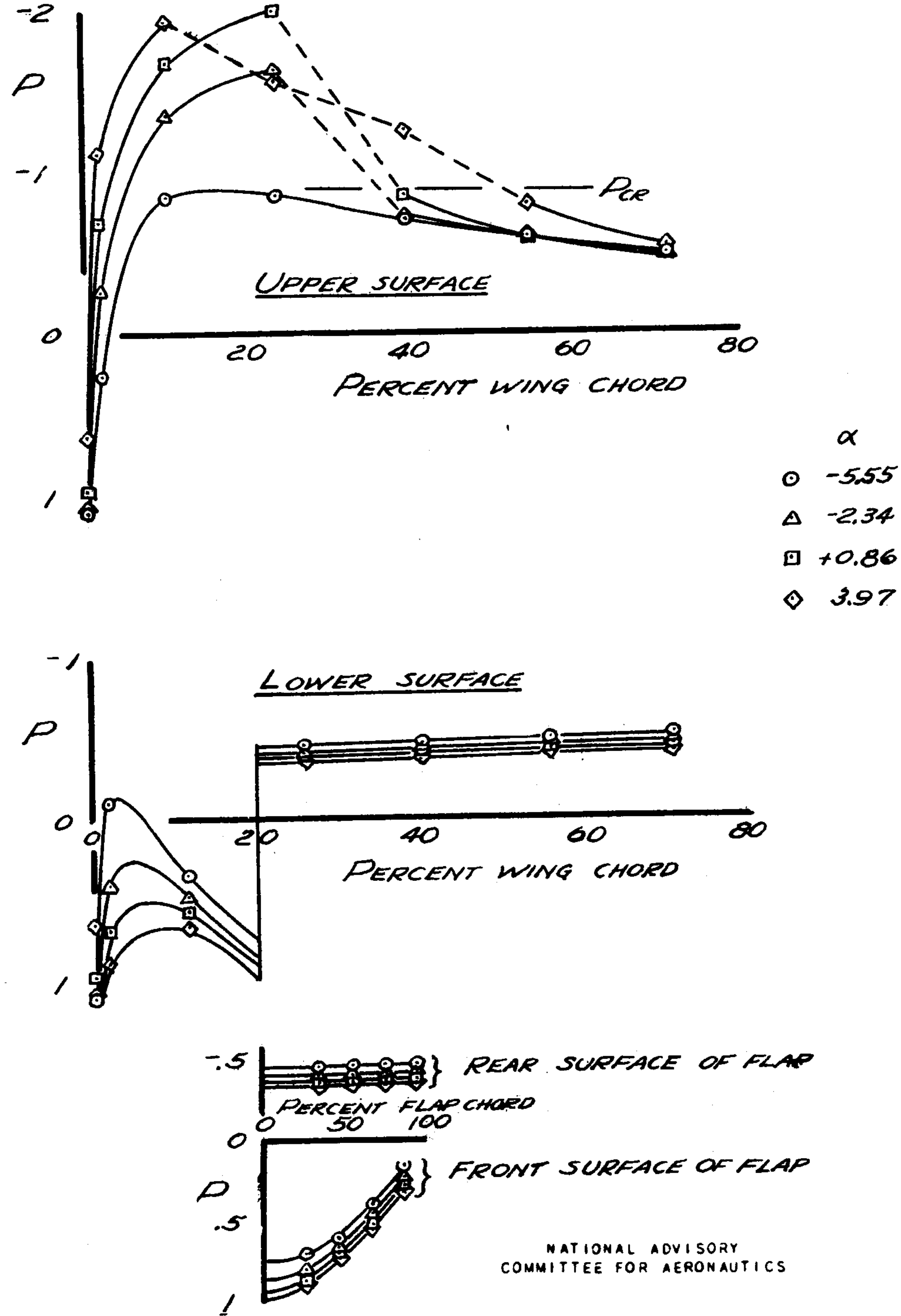

FIGURE 18(b).- WING AND FLAP PRESSURE DISTRIBUTION AT WING STATION 28.85 ON THE 230-SERIES WING WITH OUTBOARD 45° AUXILIARY CONTROL FLAPS AT 20-PERCENT WING CHORD. MACH NUMBER, 0.674.

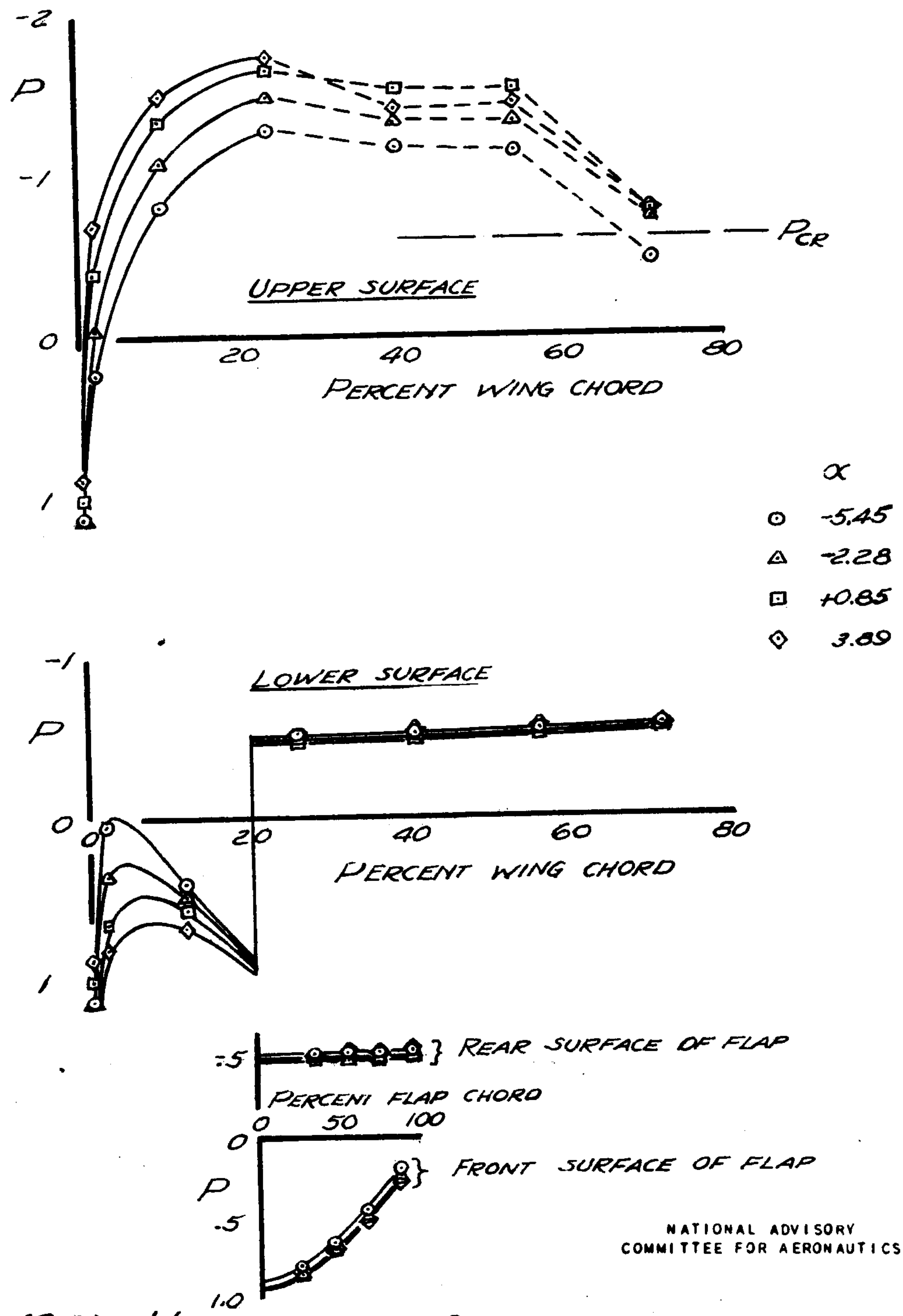

NATIONAL ADVISORY
COMMITTEE FOR AERONAUTICS

FIGURE 18 (c).- WING AND FLAP PRESSURE DISTRIBUTION AT WING STATION 28.85 ON THE 230-SERIES WING WITH OUTBOARD 45° AUXILIARY CONTROL FLAPS AT 20-PERCENT WING CHORD. MACH NUMBER, 0.747.

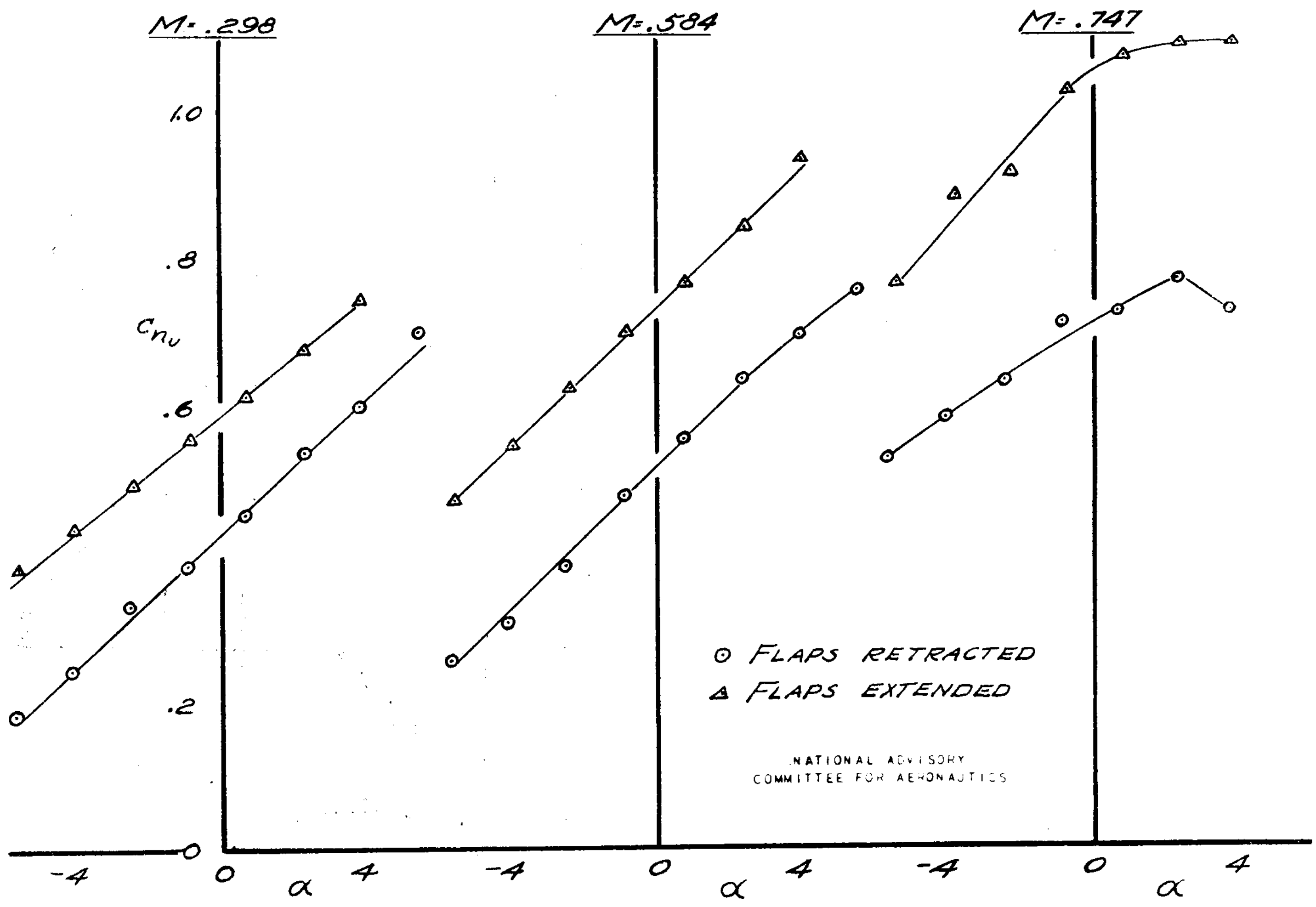

FIGURE 19(a).- SECTION NORMAL-FORCE COEFFICIENTS FROM UPPER SURFACE OF THE 230-SERIES WING WITH FLAPS RETRACTED AND WITH OUTBOARD 45° AUXILIARY CONTROL FLAPS AT 20-PERCENT WING CHORD.

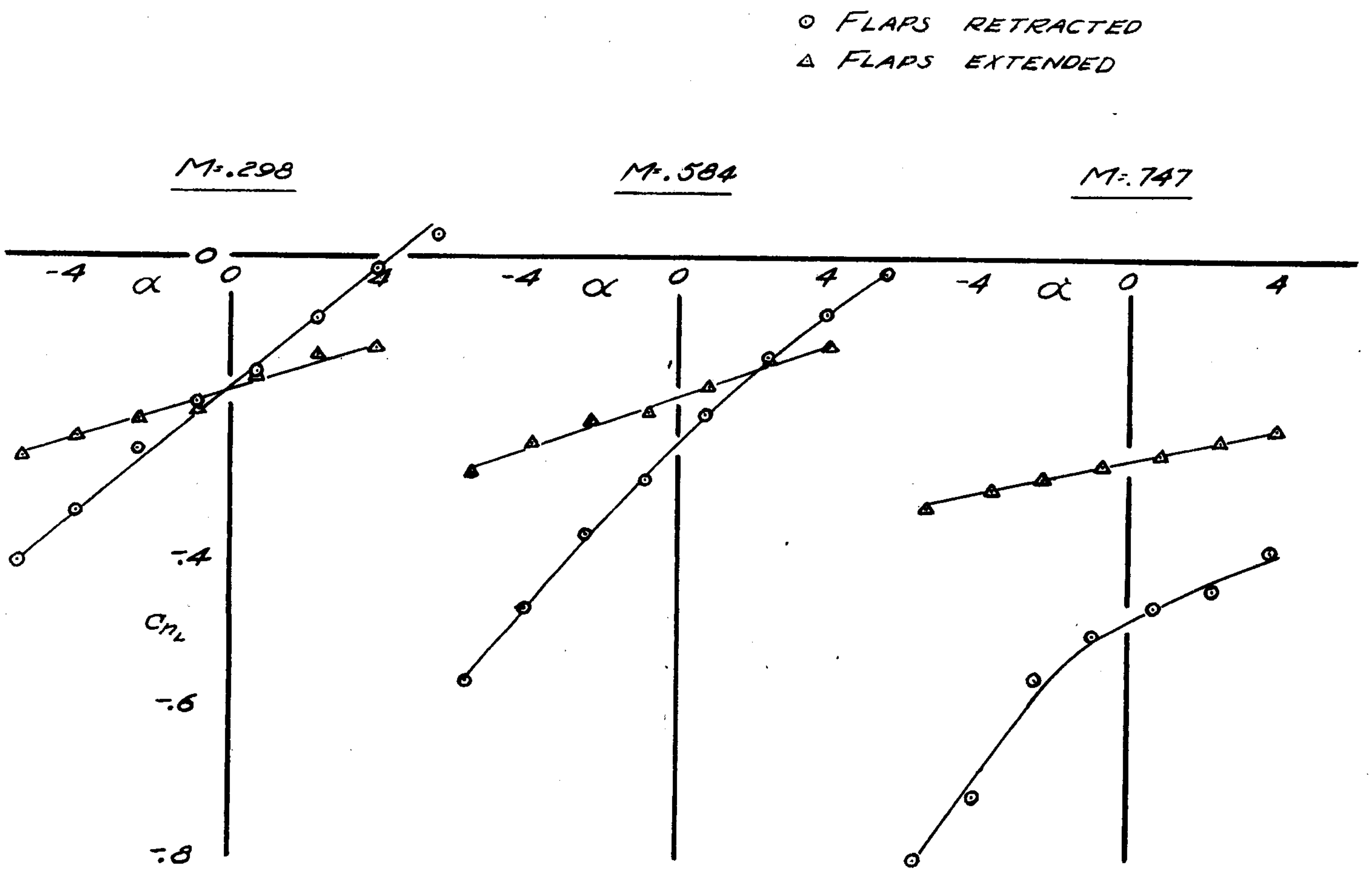

NATIONAL ADVISORY
COMMITTEE FOR AERONAUTICS

FIGURE 19(b).- SECTION NORMAL-FORCE COEFFICIENTS FROM LOWER SURFACE OF THE 230-SERIES WING WITH FLAPS RETRACTED AND WITH OUTBOARD 45° AUXILIARY CONTROL FLAPS AT 20-PERCENT WING CHORD.

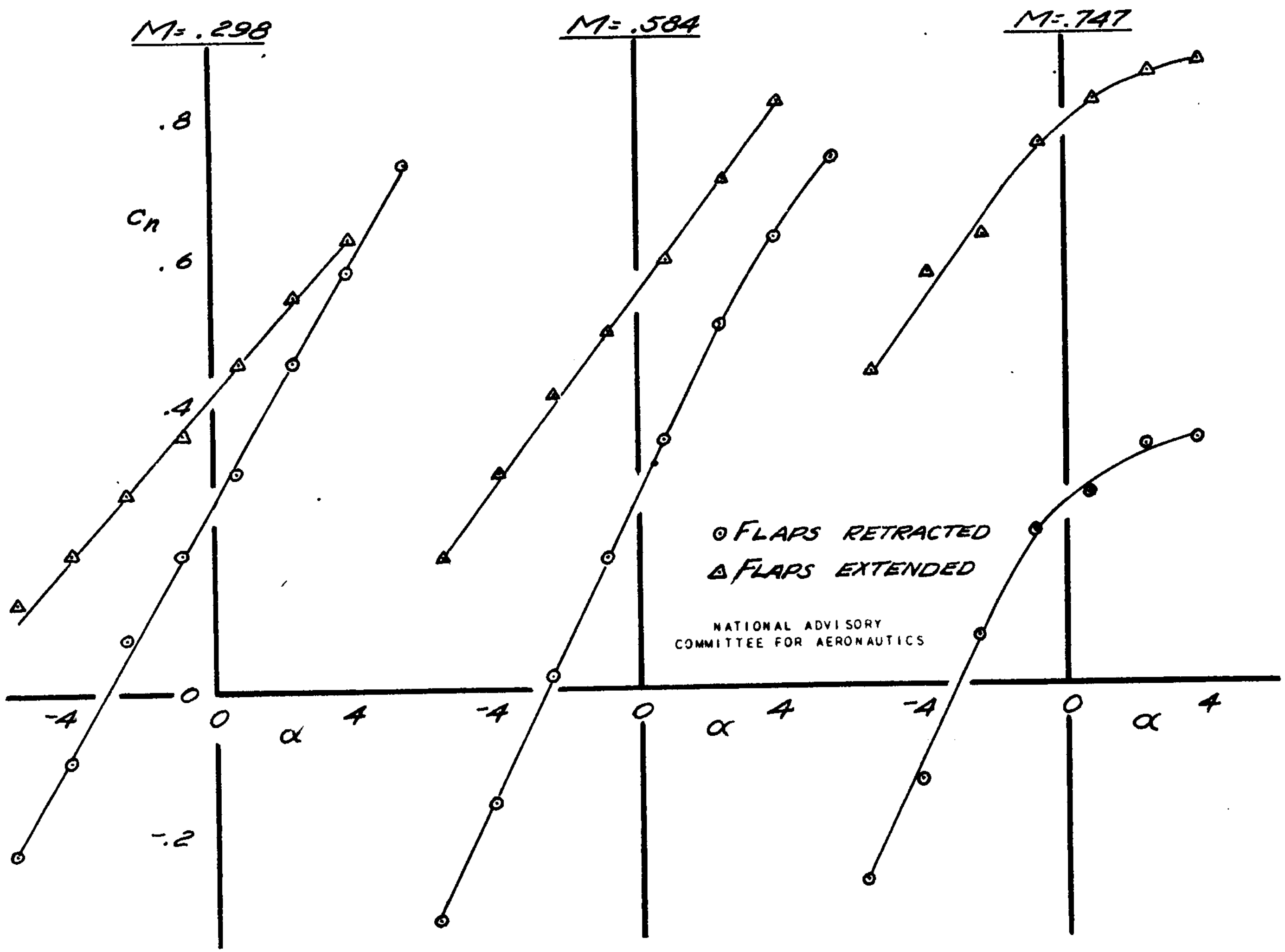

FIGURE 19(c).- SECTION NORMAL-FORCE COEFFICIENTS ON THE 230-SERIES WING WITH FLAPS RETRACTED AND WITH OUTBOARD 45° AUXILIARY CONTROL FLAPS AT 20-PERCENT WING CHORD.

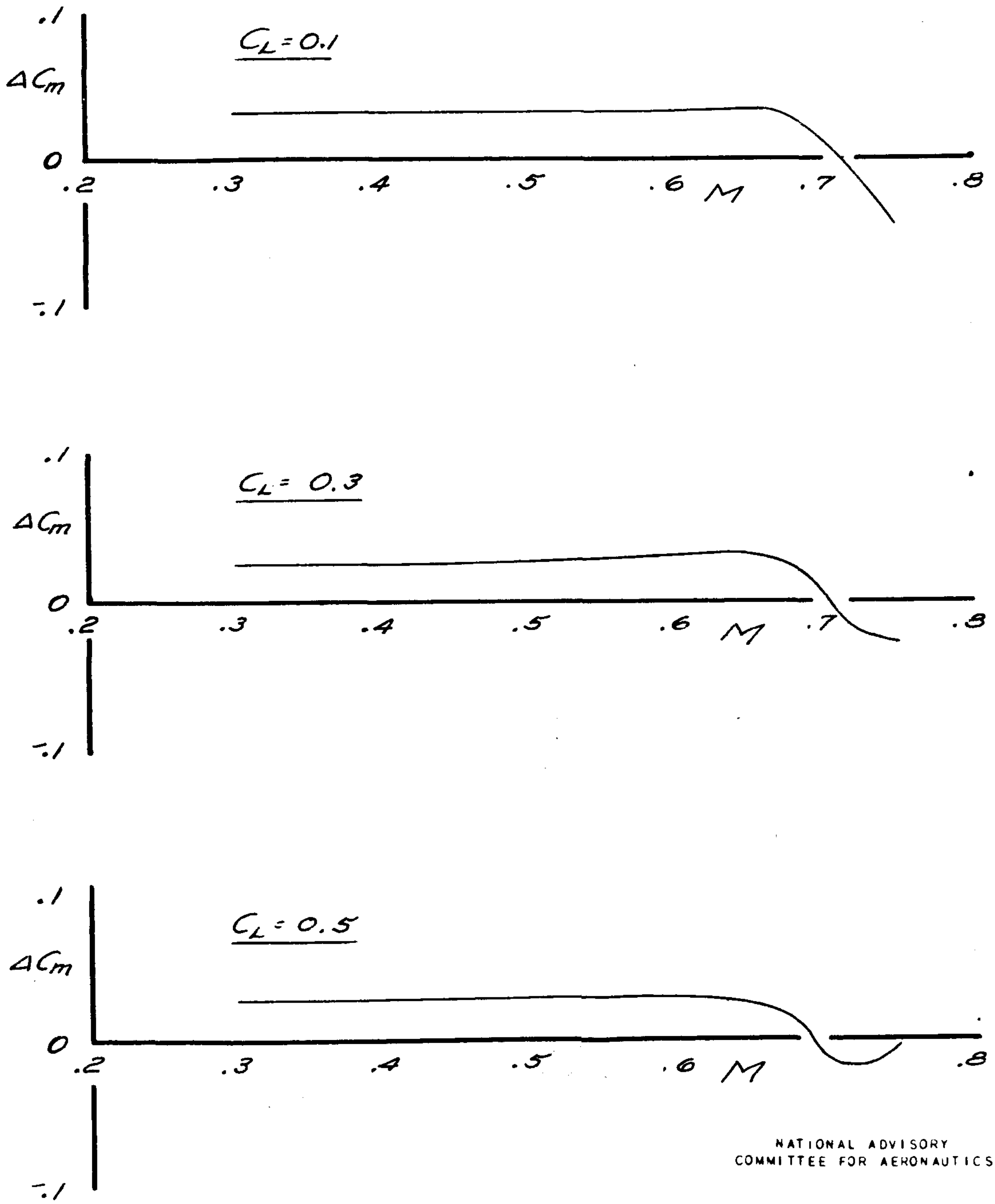

NATIONAL ADVISORY
COMMITTEE FOR AERONAUTICS

FIGURE 20. - ADDITIONAL PITCHING-MOMENT COEFFICIENT FROM THE OUTBOARD 45° AUXILIARY CONTROL FLAPS AT 30-PERCENT WING CHORD ON THE HIGHLY CAMBERED 66-SERIES WING.

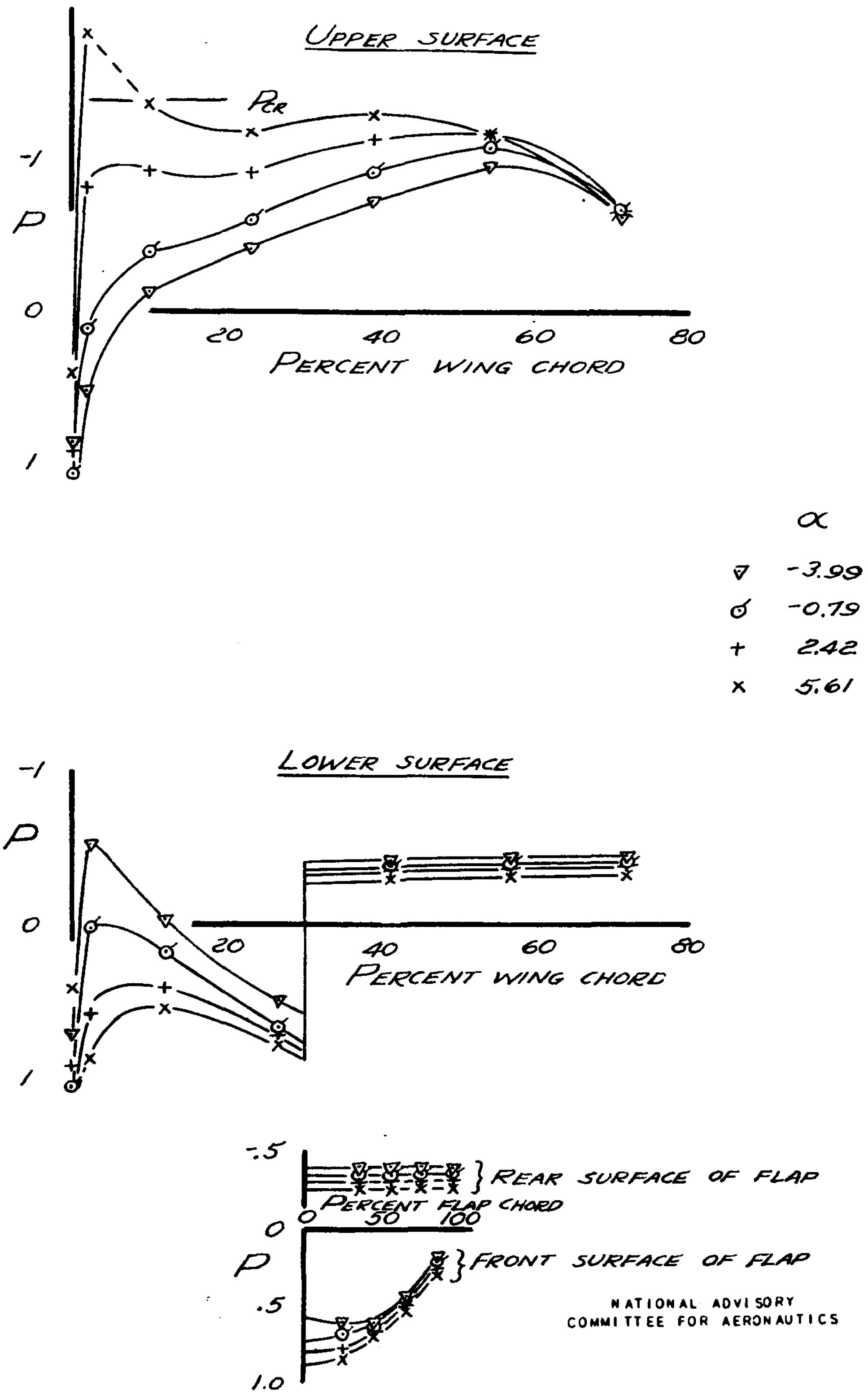

FIGURE 21 (a).- WING AND FLAP PRESSURE DISTRIBUTION AT WING STATION 28.6 ON THE HIGHLY CAMBERED 66-SERIES WING WITH OUTBOARD 45° AUXILIARY CONTROL FLAPS AT 30-PERCENT WING CHORD. MACH NUMBER, 0.584.

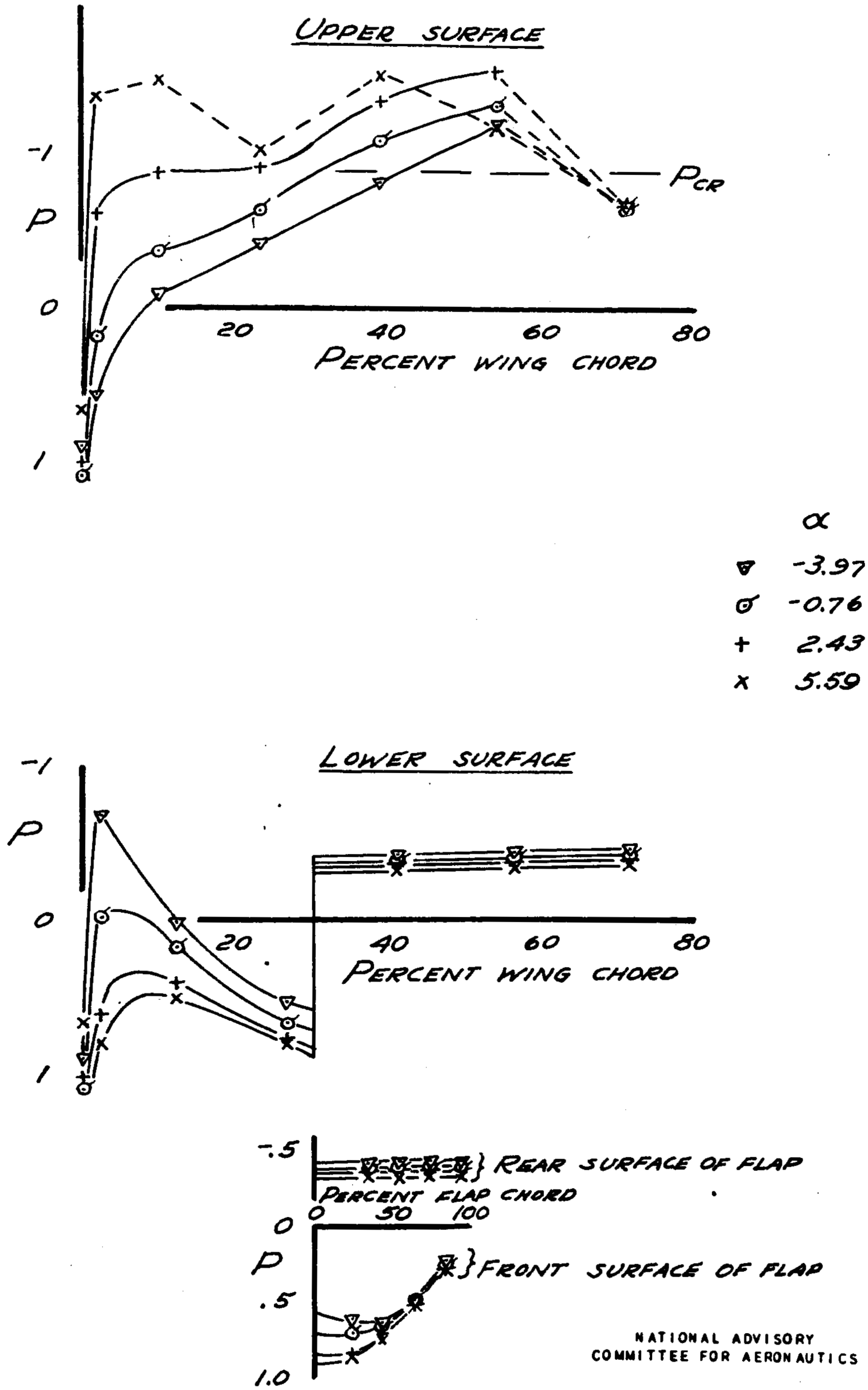

FIGURE 21(b).- WING AND FLAP PRESSURE DISTRIBUTION AT WING STATION 28.6 ON THE HIGHLY CAMBERED 66-SERIES WING WITH OUTBOARD 45° AUXILIARY CONTROL FLAPS AT 30-PERCENT WING CHORD. MACH NUMBER, 0.674.

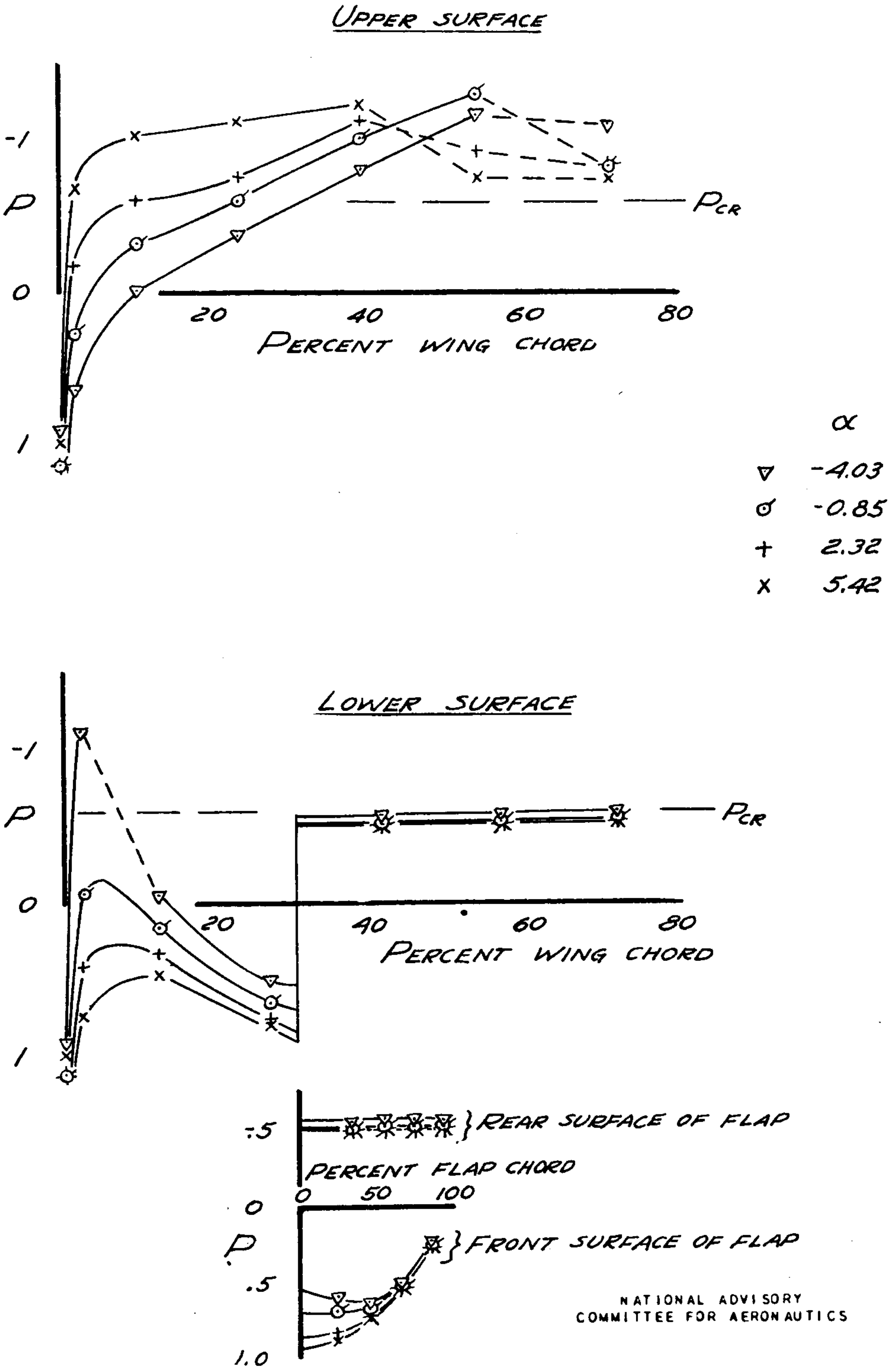

NATIONAL ADVISORY COMMITTEE FOR AERONAUTICS

FIGURE 21(c).- WING AND FLAP PRESSURE DISTRIBUTION AT WING STATION 28.6 ON THE HIGHLY CAMBERED 66-SERIES WING WITH OUTBOARD 45° AUXILIARY CONTROL FLAPS AT 30-PERCENT WING CHORD. MACH NUMBER, 0.747.

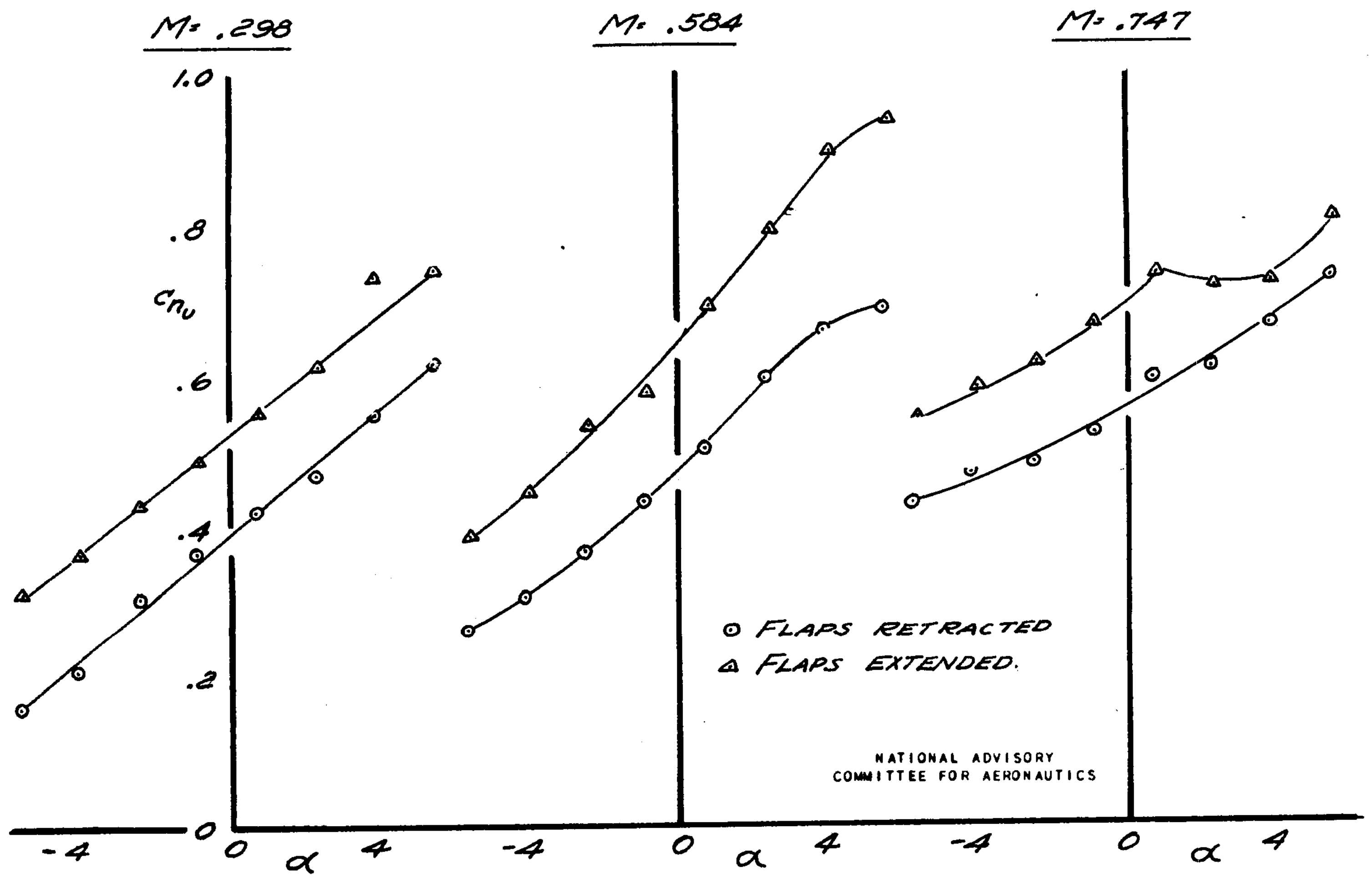

FIGURE 22 (a). - SECTION NORMAL-FORCE COEFFICIENTS FROM THE UPPER SURFACE OF THE HIGHLY CAMBERED 66-SERIES WING WITH FLAPS RETRACTED AND WITH OUTBOARD 45° AUXILIARY CONTROL FLAPS AT 30-PERCENT WING CHORD.

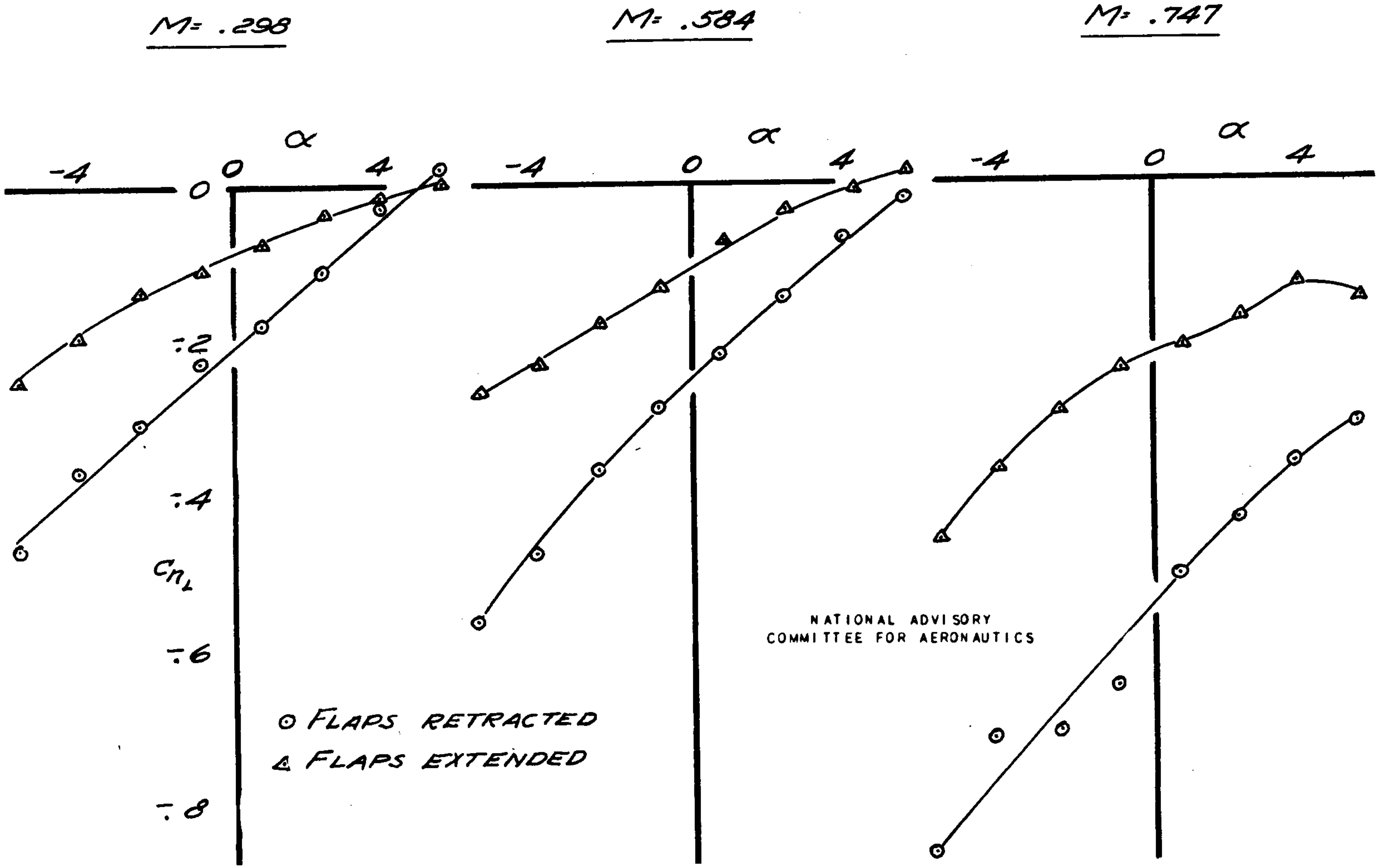

FIGURE 22 (b).- SECTION NORMAL-FORCE COEFFICIENTS FROM THE LOWER SURFACE OF THE HIGHLY CAMBERED 66-SERIES WING WITH FLAPS RETRACTED AND WITH OUTBOARD 45° AUXILIARY CONTROL FLAPS AT 30-PERCENT WING CHORD.

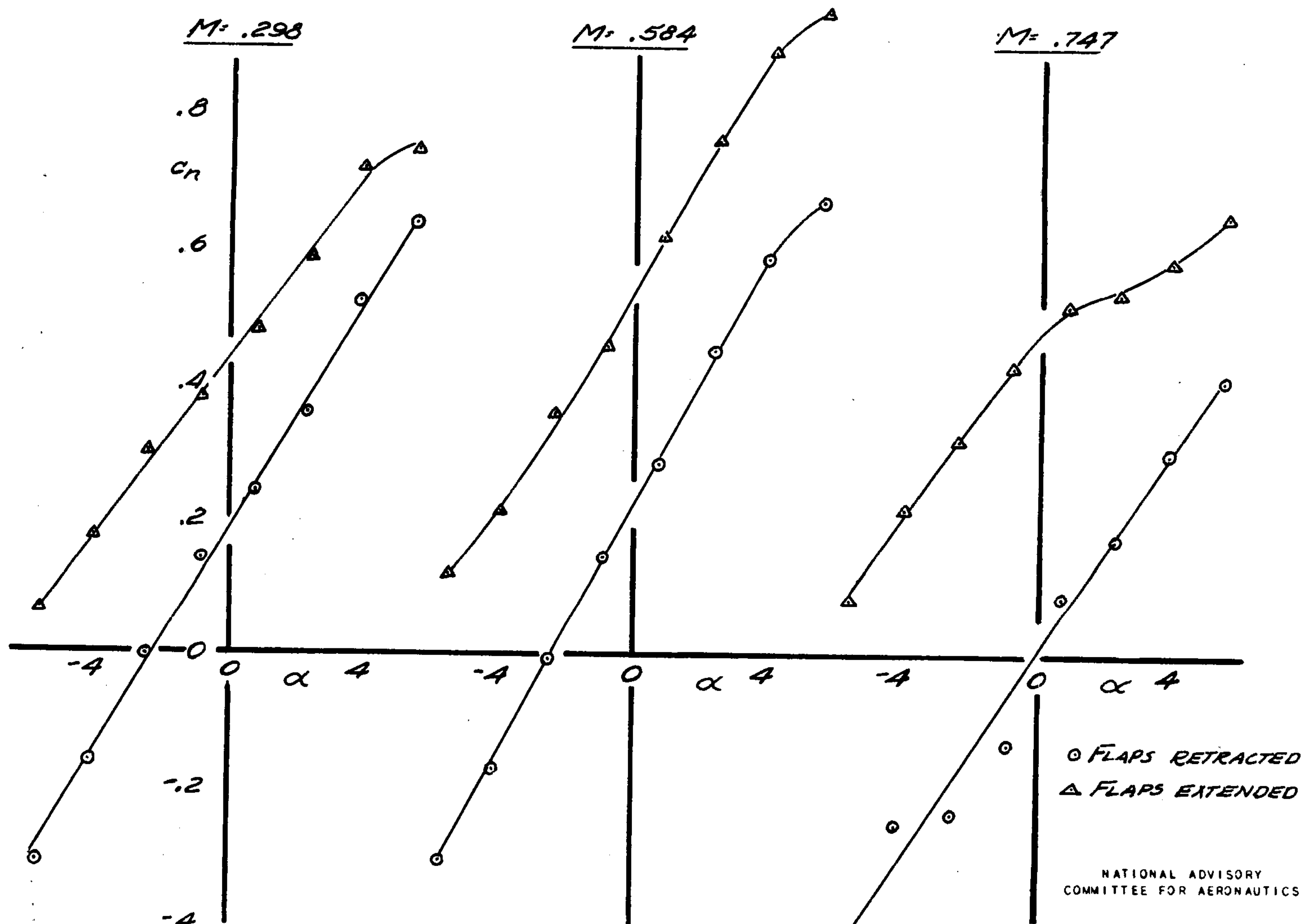

NATIONAL ADVISORY COMMITTEE FOR AERONAUTICS

Figure 22 (c).- Section normal-force coefficients on the highly cambered 66-series wing with flaps retracted and with outboard 45° auxiliary control flaps at 30-percent wing chord.

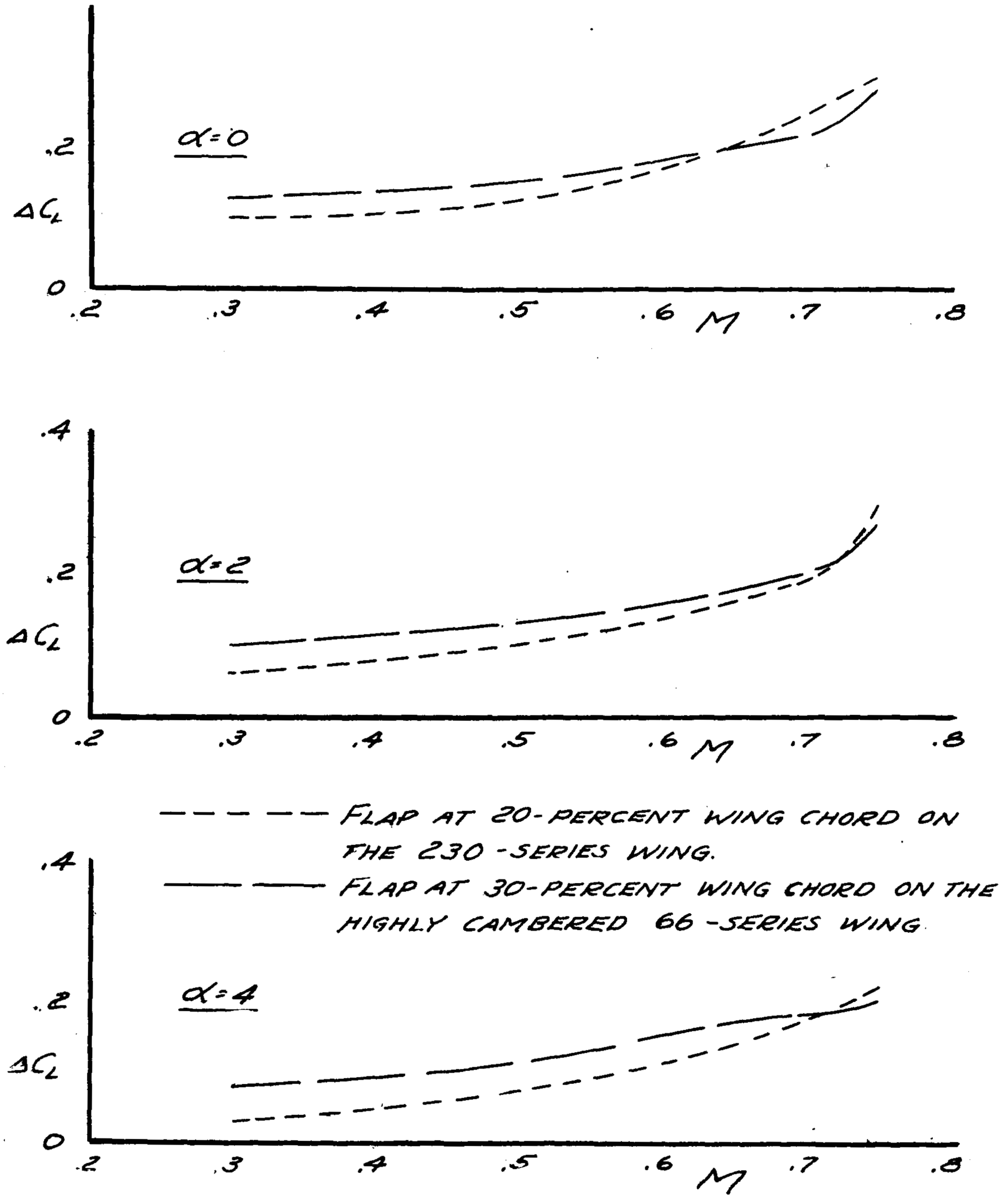

NATIONAL ADVISORY
COMMITTEE FOR AERONAUTICS

FIGURE 23.- ADDITIONAL LIFT COEFFICIENT FROM THE OUTBOARD 45° AUXILIARY CONTROL FLAPS.

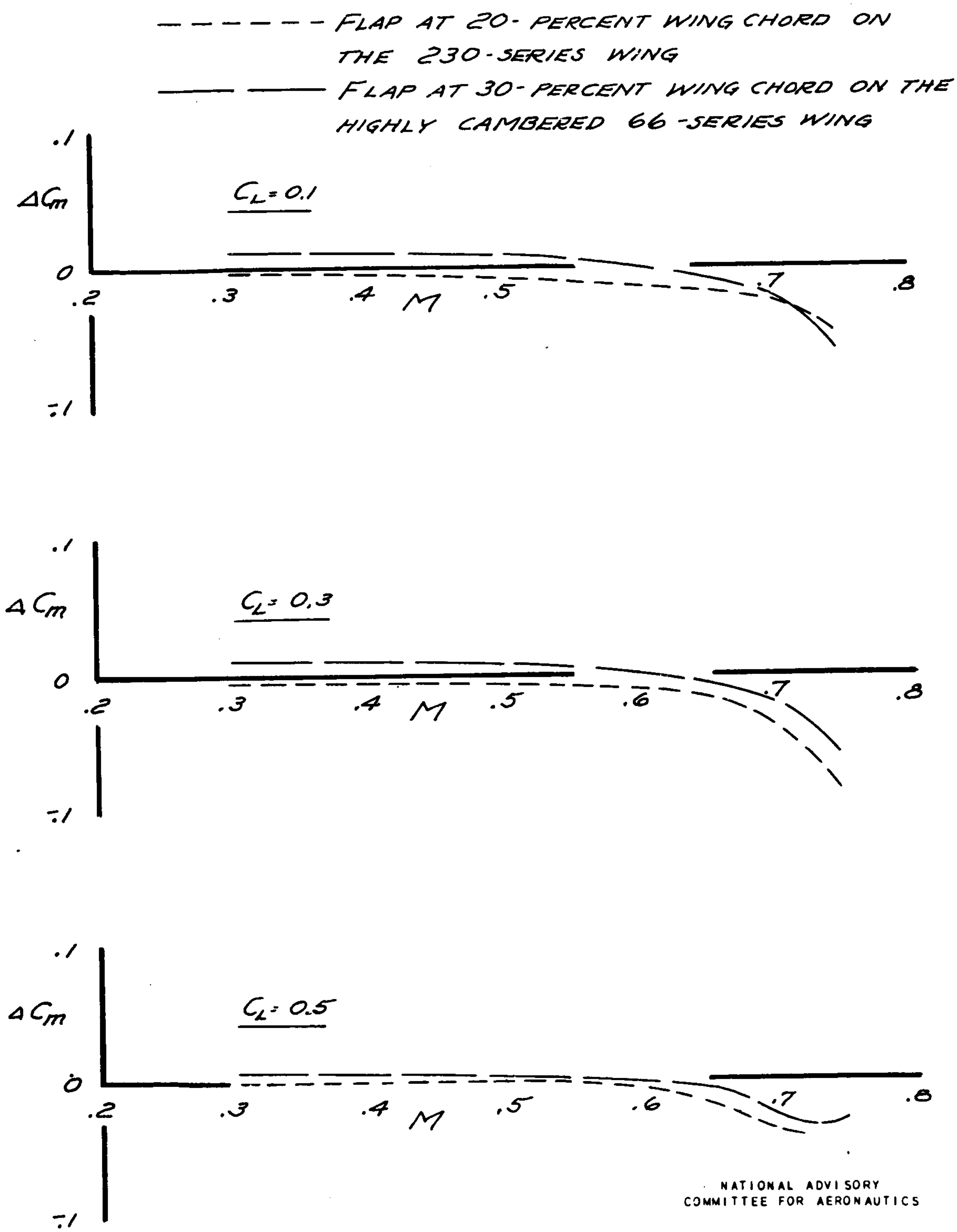

NATIONAL ADVISORY COMMITTEE FOR AERONAUTICS

FIGURE 24.- ADDITIONAL PITCHING-MOMENT COEFFICIENT FROM THE OUTBOARD 45° AUXILIARY CONTROL FLAPS WITH TAIL OFF.

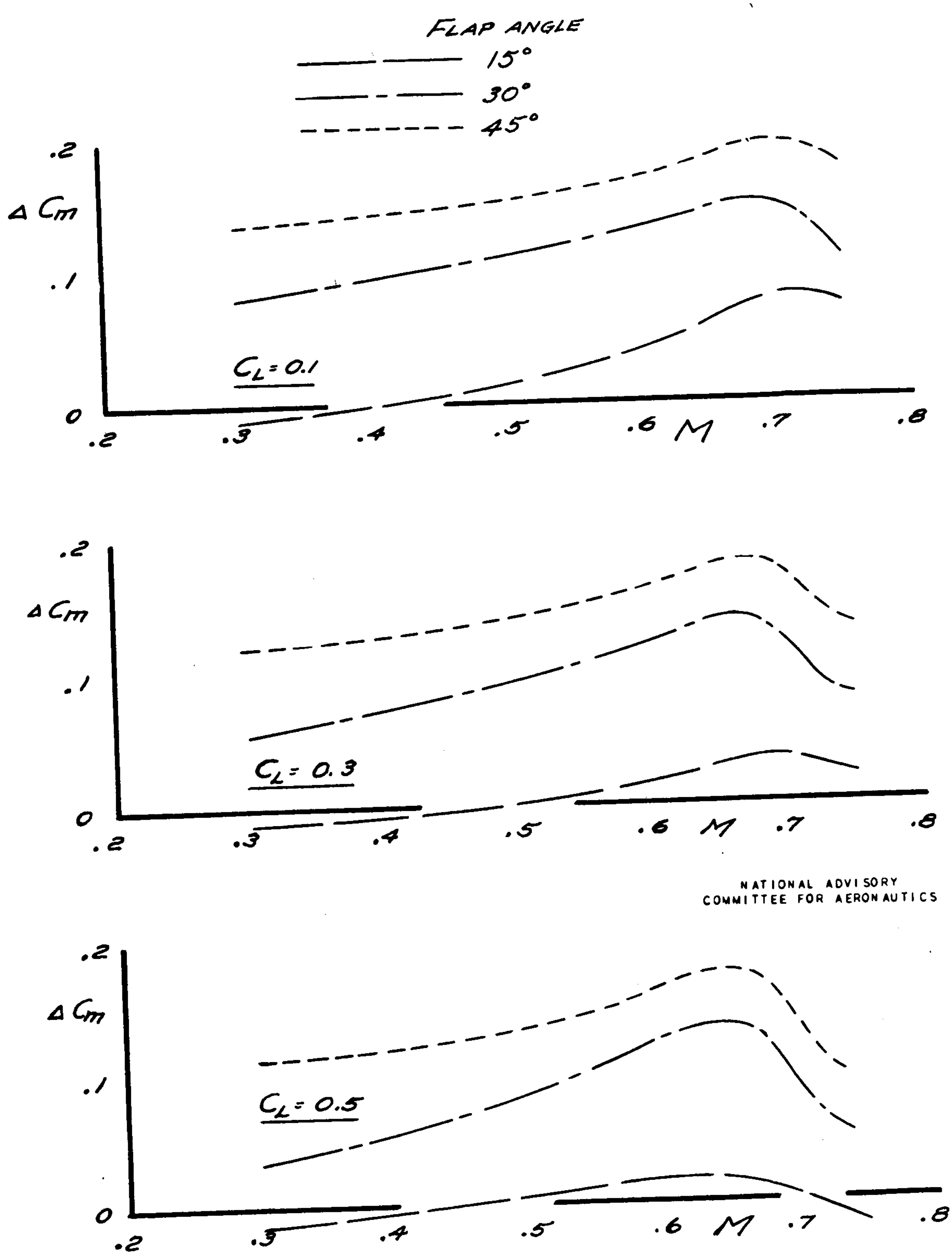

FIGURE 25.- ADDITIONAL PITCHING-MOMENT COEFFICIENT FROM VARIOUS DEFLECTIONS OF THE INBOARD AUXILIARY CONTROL FLAPS AT 30-PERCENT WING CHORD ON THE HIGHLY CAMBERED 66-SERIES WING.

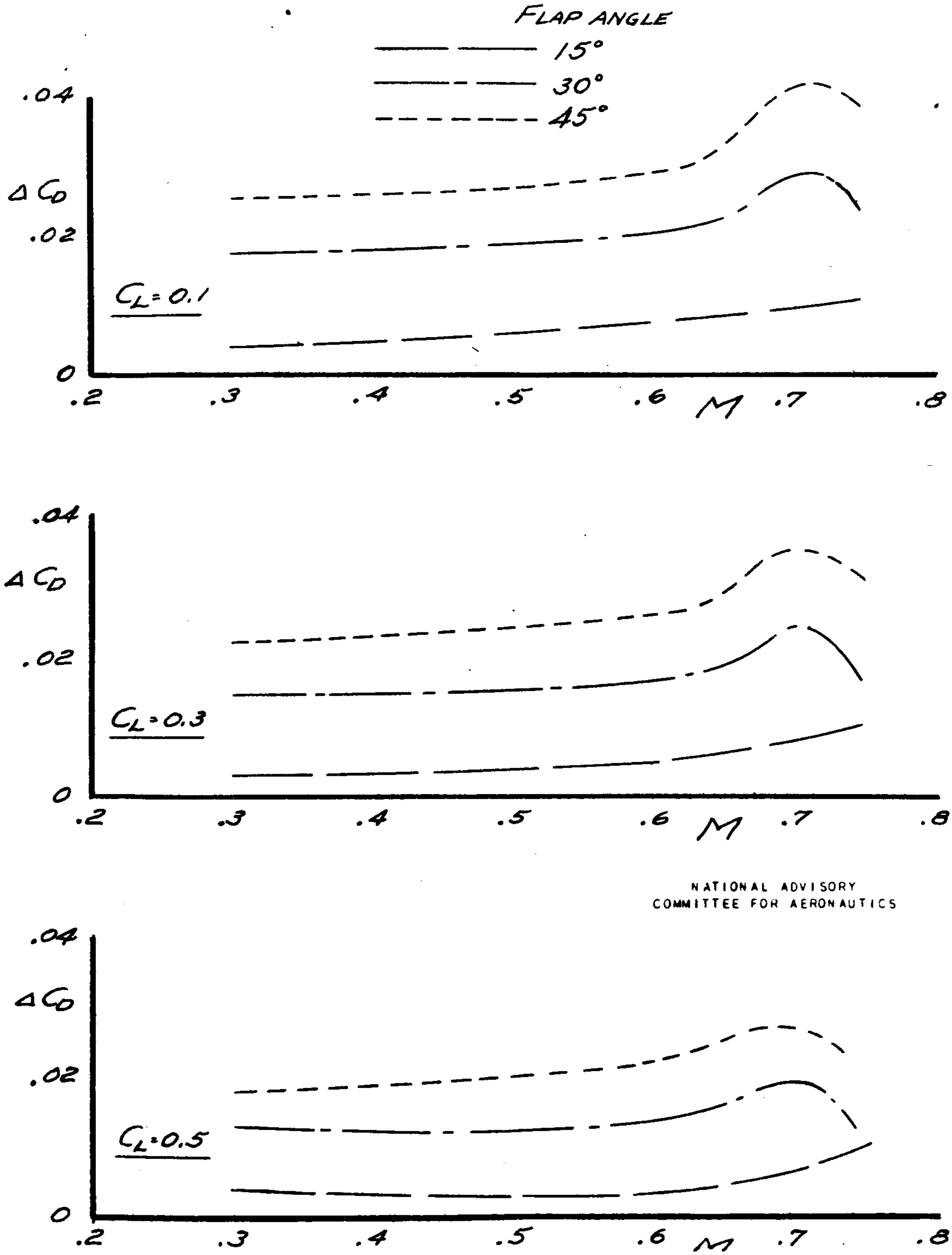

FIGURE 26.- ADDITIONAL DRAG COEFFICIENT FROM VARIOUS DEFLECTIONS OF THE INBOARD AUXILIARY CONTROL FLAPS AT 30-PERCENT WING CHORD ON THE HIGHLY CAMBERED 66-SERIES WING.

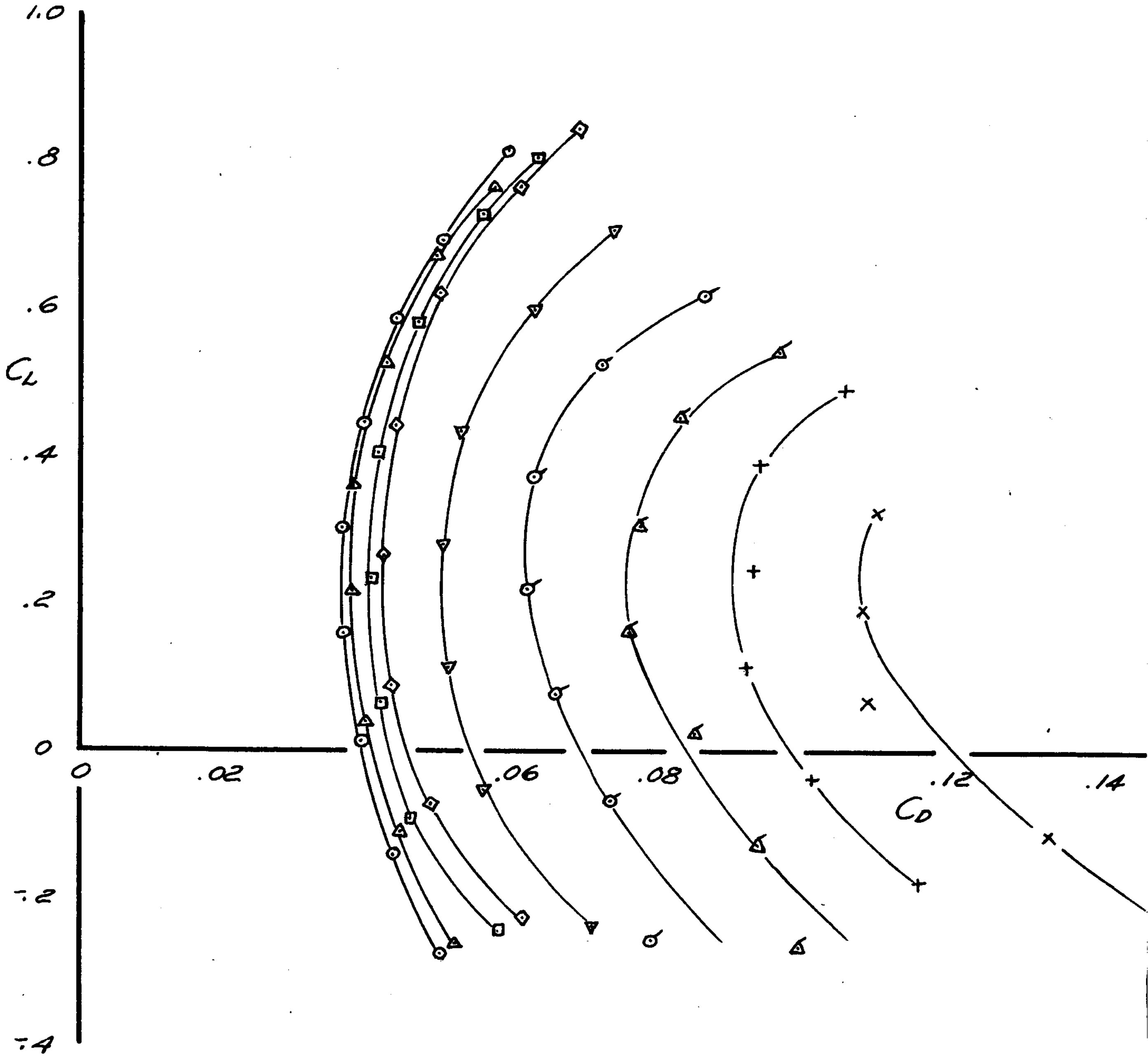

FIGURE 27A

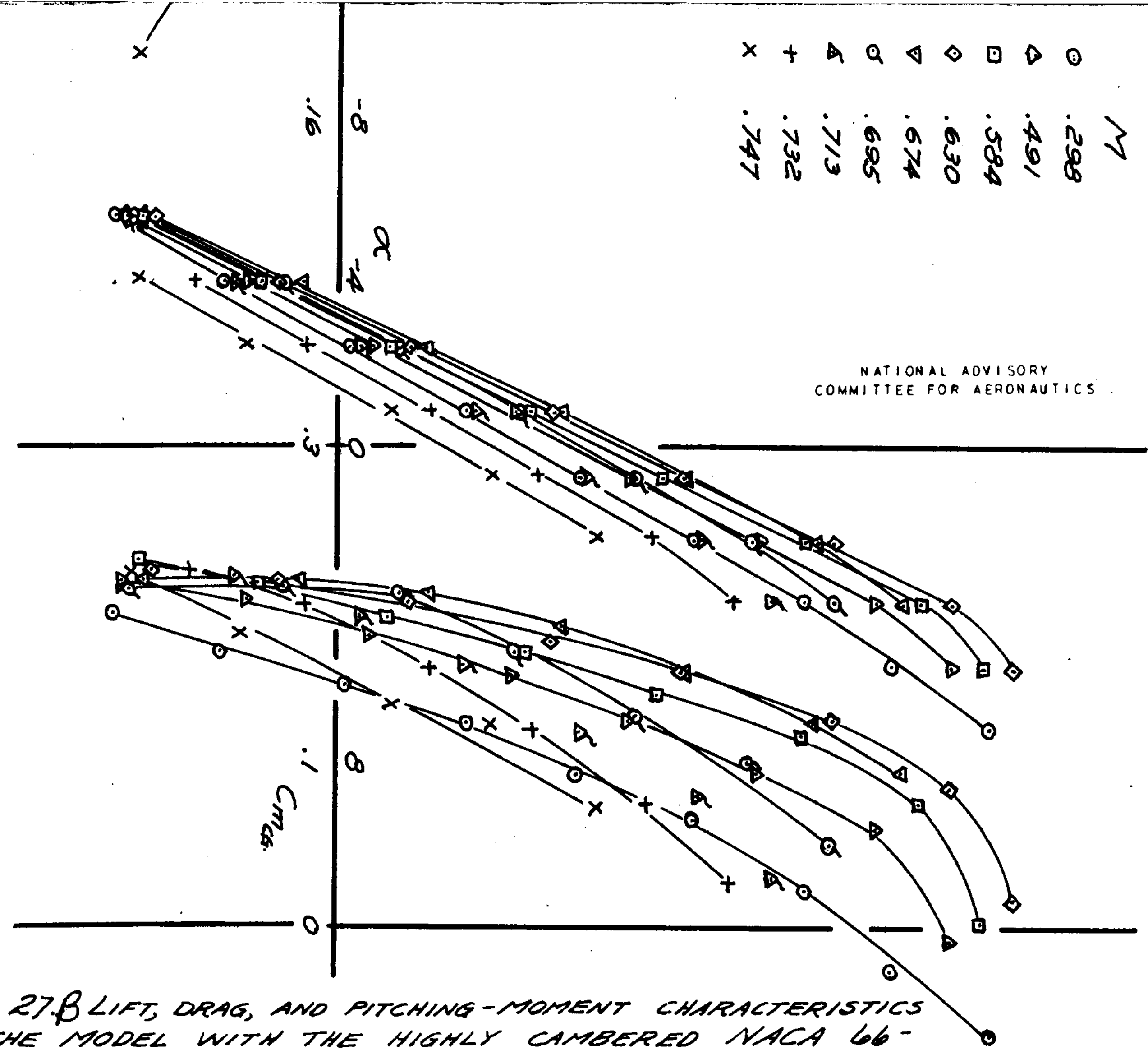

FIGURE 27.B LIFT, DRAG, AND PITCHING-MOMENT CHARACTERISTICS OF THE MODEL WITH THE HIGHLY CAMBERED NACA 66-SERIES. WING AND INBOARD 30° AUXILIARY CONTROL FLAPS AT 30-PERCENT WING CHORD. STABILIZER ANGLE, 0°.

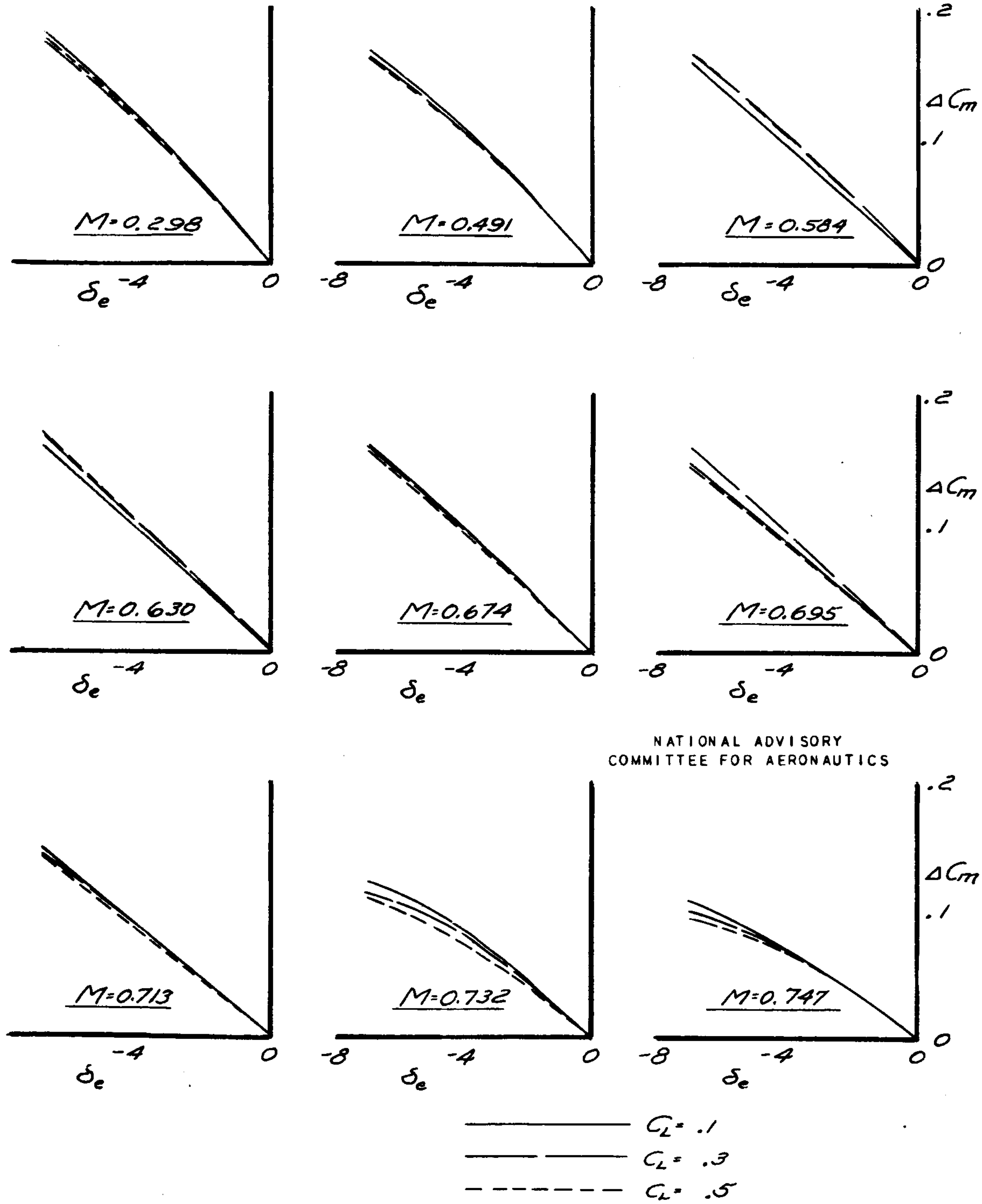

FIGURE 28.- ADDITIONAL PITCHING-MOMENT COEFFICIENT FROM DEFLECTION OF THE ELEVATOR. MODEL WITH THE HIGHLY CAMBERED 66-SERIES WING.

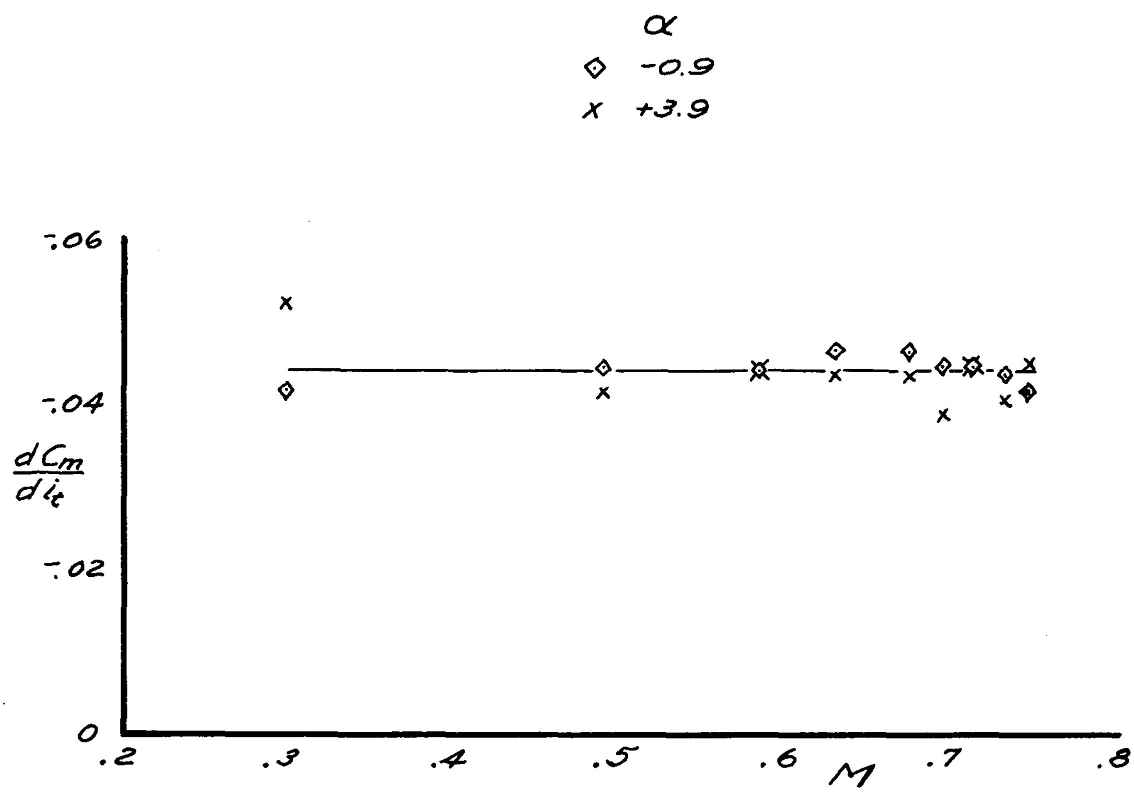

NATIONAL ADVISORY COMMITTEE FOR AERONAUTICS

FIGURE 29.- VARIATION OF STABILIZER EFFECTIVENESS WITH MACH NUMBER. MODEL WITH THE HIGHLY CAMBERED 66-SERIES WING.